Journal of Thermal Analysis and Calorimetry, Vol. 89 (2007) 2, 321–356

THERMAL ANALYSIS OF MACROMOLECULES
A personal review

B. Wunderlich[1,2**]

[1]Department of Chemistry, University of Tennessee, Knoxville, TN 37996-1600, USA
[2]Chemical Sciences Division, Oak Ridge National Laboratory, Oak Ridge, TN 37831-6197, USA

This review traces the development of thermal analysis over the last 50 years as it was experienced and contributed to by the author. The article touches upon the beginning of calorimetry and thermal analysis of polymers, the development of differential scanning calorimetry (DSC), single-run DSC, and other special instrumentations, up to the recent addition of modulation to calorimetry and superfast calorimetry.

Many new words and phrases have been introduced to the field by the author and his students, leaving a trail of the varied interests over 50 years. It began with cold crystallization and more recently the terms oriented, intermediate phase, glass transitions of crystals, and decoupled chain segments were coined. In-between the following phenomena were named and studied: extended-chain crystals, irreversible thermodynamics of melting of polymer crystals, zero-entropy-production melting, dynamic differential thermal analysis (DDTA), the rule of constant increase of C_p per mobile bead within a molecule at the glass transition temperature, superheating of polymer crystals, melting kinetics, crystallization during polymerization, chain-folding principle, molecular nucleation, rigid amorphous phase, system of classifying molecules, macroconformations, amorphous defects, rules for the entropy of fusion based on molecular shape and flexibility, single-molecule single-crystals, systems for classifying phases and mesophases including condis phases, and the globally metastable semicrystalline polymers with reversible, local subsystems.

Keywords: *DSC, fifty-year review, macromolecules, molecular motion, nonequilibrium, phases, thermal analysis, thermodynamics, TMDSC*

A brief biography

It is a special honor to be asked to add a personal review of thermal analysis of macromolecules to this special symposium issue of the Proceedings of the 34th NATAS Conference which recognizes my 75th birthday. At the same time, this is also the 60th anniversary of my interest in Chemistry and the 50th anniversary of the beginning of my work in thermal analysis and polymer science. It is amazing how fast time passes when one has fun with what one is doing.[*]

It all began somewhat sadly with the bombing of the house of my parents on April 20, 1945 in Brandenburg, Germany. Fortunately the family was not at home. We were refugees in the forests nearby. After the war had ended and some degree of normalcy had returned, school started again in the Fall of 1945, but my goal to become a farmer needed to be revised due to the land reform introduced in East Germany. It took my prospective farm and left no other choice but to continue my education through high school.

In 1946 I discovered chemistry by reading the 9th edition of U. Hofmann's 'Inorganic Chemistry'. The book had ended up the year before in my collection when the two floors of our apartment building collapsed during the bombing. Our neighbor, who used the book in his studies, thought I might enjoy studying it. I did. What an enormous source of interesting facts and historical footnotes! Later, I could use the same textbook at the University of Berlin (Humboldt University, 1949–53) as the basic study guide. In 1947, chemistry was introduced as a high-school subject, and being properly primed, I made it quickly to the top of the class in this subject, and ultimately chose it for my university study in 1949. The 14th edition of Hofmann (and Ruedorf) is still on my book shelf and over the years has answered many questions in chemistry.

The beginning of the university study was, again, not without some problems. It took the forceful intervention of Prof. E. Thilo of the Humboldt University to overcome the problem that I did not belong

---

[*] This review is an update of a publication written in 1995 and published under the same title in the J. Thermal Anal., 46 (1996) 643. Parts F and G are fully new, and Part G is the basis for my lecture: 'The development of the idea of thermodynamic decoupling in macromolecules'.

[**] Wunderlich@CharterTN.net

1388–6150/$20.00

Akadémiai Kiadó, Budapest, Hungary
Springer, Dordrecht, The Netherlands

to the preferred class of workers and peasants and was not politically active. Besides teaching me how to teach chemistry, Prof. Thilo instilled an interest in phosphates and silicates. Many years later a student of mine and I could contribute some new knowledge about ‘crystallization during polymerization’ of LiH_2PO_4, using thermogravimetry (TG) and differential scanning calorimetry (DSC) [1].

After four years, my wish to solely study chemistry and avoid politics made me a refugee again [on June 17, 1953, the date of the uprising in the GDR (East Germany)]. With Prof. Thilo’s help I could at least extract my proof of study from Berlin. After a few months in refugee camps and work at the Farbwerke Hoechst, I continued studying chemistry for two semesters at the Goethe University in Frankfurt, got married in the famous City Hall (the Römer), and emigrated to the United States.

Two semesters of study at Hastings College in Hastings, NE taught me everything needed to enter graduate school as Research Assistant to Prof. Malcolm Dole at Northwestern University in Evanston, IL. The subject of study was calorimetry of polymers. It was a very opportune time for this topic. Polymers was still a relatively new subject, taught at very few universities, and calorimetry has always been a topic for only a select few researchers. Prof. Dole, being a former coworker in Prof. Debye’s Institute in Leipzig, Germany in 1929, and having gained interest in polymers already before WW II, was the unique expert in the field to educate students [2]. Under his expert guidance, it (only) took until 1957 to complete my Ph.D. thesis on the ‘Thermodynamics of the Copolymer System Poly(ethylene terephthalate-sebacate)’ [3, 4]. Besides the actual heat capacity measurements, the process of ‘cold crystallization’ was recognized and named. It occurs somewhat above the glass transition temperature as the limiting non-equilibrium mode of crystallization. During a subsequent year as Instructor at Northwestern University, the kinetics, thermodynamics, and statistics of the non-equilibrium cold crystallization and melting were analyzed with help of the, at that time, revolutionary and brand new electronic calculator (IBM 650) [5]. Figure 1 illustrates the broad area of possible non-equilibrium crystallinity if one assumes that cold crystallization in polyterephthalates is limited to nanocrystals of three repeating units in length (»3 nanometers).

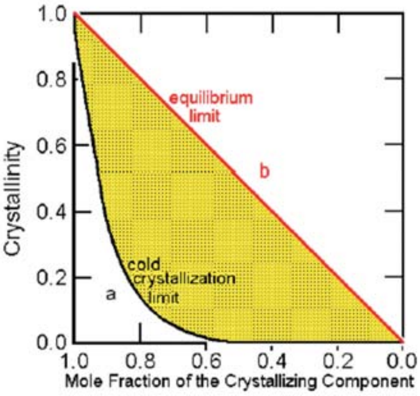

Fig. 1 Mole fraction of crystallinity, w_c, of component A in poly(A-co-B) after cold crystallization as function of mole fraction of component A. Curve a is the lower limit of non-equilibrium crystallinity. Curve b indicates the equilibrium crystallinity [5]

Many of the present research topics of our Advanced THermal Analysis System and Laboratory, ATHAS, have their roots in this first look at the thermal properties of polymers. Further early work was carried out at Cornell University where I was an instructor and later assistant professor in the Department of Chemistry from 1958 to 1963 (‘Early calorimetry and knowledge about solid polymers (1955–1965)’, below). The main body of research was generated during my 25-year tenure at Rensselaer Polytechnic Institute (1963–88) as Professor of Chemistry (promotion to full professor in 1965) (‘First DSC and morphology (1965–1975)’ and ‘Computerization and formal development of ATHAS (1975–1988)’). After early retirement from RPI, the next stage of research was begun at The University of Tennessee and at Oak Ridge National Laboratory (1988–2001). This work is covered in ‘Molecular motion and disorder (1988–1996)’ and ‘Reversible melting and the rigid-amorphous phase (1996–2003)’ and after retirement was continued to the present day by building on all prior experience (‘Reversible melting and the rigid-amorphous phase (1996–2003)’ and ‘Decoupling of chain segments of flexible macromolecules (2003–)’). The idea of the ATHAS was generated in the mid 1970s and has ever since been the focus of the research of my students and postdoctoral fellows. At present, the ATHAS Laboratory is moved by Dr. Marek Pyda, my last postdoctoral research associate, and from 2001–06 Director of the ATHAS Laboratory, to the Department of Chemistry at the University of Technology in Rzeszow, Poland. It is hoped that by this move, the ATHAS information will remain available to the thermal analysis community and grow for the benefit of everyone.

Early calorimetry and knowledge about solid polymers (1955–1965)

Most calorimetry on polymers in this early time period was done by adiabatic calorimetry. The instrumentation was based on the classical design of Nernst [6]. Major calorimeters were only in operation at the Bureau of Standards [7] (now NIST) and

Prof. Dole's laboratory [8]. During this decade these two major producers of data on polymers were joined by the GE Research Laboratory (Karasz *et al*. [9]) and work was begun at the University of Leeds, England (Dainton *et al*. [10]). A check of the literature [11] revealed that through 1955 only 30 papers on heat capacity of linear macromolecules were published, describing mainly natural and synthetic rubbers, polystyrene, poly(vinyl chloride), polyethylene, selenium, nylon-6, poly(tetrafluoroethylene), and poly(fluorotrichloroethylene). The first papers on heat capacity of characterized polymers date back to 1928 [12], 1935 [13], 1937 [14] and 1938 [15]. The basis of the theory of heat capacity of solids was given by Einstein [16] and Debye [17], and an extension to polymers was suggested by Tarasov [18]. A detailed analysis of the vibrational characteristics of a polymer was suggested by Stockmayer and Hecht [19]. This means, at that time a solid foundation existed for the growth of knowledge about the thermal properties of polymers. The major limitations were that most attempts to understand these thermal properties of macromolecules made use of an equilibrium approach and that the morphology of polymer crystals was not well understood.

The knowledge of flexible macromolecules in the solid-state underwent a dramatic change in this time period. Polymers with rather regular chemical structure were known to crystallize, but only partially. Less regular polymers were glassy at sufficiently low temperature. Both states of matter are not in equilibrium. With the help of electron microscopy it could be shown in 1955 by Keller, Fischer, Till and Kobayashi that flexible macromolecules are prone to crystallize in a lamellar morphology [20, 21]. The polymer molecules are much longer than the lamellae are thick and fold or leave the crystal phase at the lamellar surface. The lamellar thickness (fold length) was found to be 5–50 nm, making the crystals highly metastable. Optical interference microscopy [22] was developed in our laboratory for quantitative analysis of the morphology and measurement of lamellar thickness [23]. Extending the measurements to solution grown single crystals produced at pressures up to 600 MPa gave experimental proof that the reason for chain folding was kinetic and not thermodynamic. By covering a 100 K range of crystallization temperatures, the lamellar thickness was found to change with supercooling and not with temperature [24].

The experience with crystallization under elevated pressure led to the discovery of 'extended chain crystals' of polyethylene [25]. At pressures above about 300 MPa, linear polyethylene melts would, after crystallization to folded-chain lamellae, anneal to a thickness that could reach the molecular lengths of typically 1–10 μm and also achieve close to 100% crystallinity. These observations meant that, given the right experimental conditions, the whole spectrum from metastable to equilibrium crystals could be produced and was in need to be studied by thermal analysis.

For thermal analysis it was necessary to learn how to deal with the metastability of solid polymers. As the melting point is approached, annealing, reorganization and recrystallization to higher stability is possible, i.e. the sample may change during calorimetry. The first solutions were to run calorimeters as fast as possible and avoid the intermittent stops needed for regaining equilibrium [26, 27]. The next step was to build new calorimeters for smaller masses adapted better to continuous heating [28]. Finally, in 1960, continuous differential calorimetry for masses as little as one gram, and with heating rates as fast as 1.0 K min^{-1} was demonstrated by Müller and Martin [29]. About five years later, two radically new commercial calorimeters were introduced, the differential scanning calorimeters (DSC) by the Perkin-Elmer Corp. Norwalk, CT [30] and the DuPont Instrument Division, Wilmington DE (now TA Instruments, Inc.). These instruments permitted quantitative measurements for masses as little as 10 mg and with heating rates as fast as 40 K min^{-1}. Such DSCs are the principal tools for the analysis of metastable and unstable states.

Before the development of commercial DSCs we adapted differential thermal analysis, DTA, to the measurement of heat (calorimetry) [31], as we had adapted before the calorimeter to measure heat continuously [26]. For the first time it became possible to show by thermal analysis that the unusually large specific surface free energy (J g^{-1}) of the thin lamellar crystals of polyethylene can cause a substantial decrease in melting temperature [31]. It could also be proven that the fold surfaces introduced additional, and often the major melting point lowering in copolymers [32]. This insight into the 'irreversible thermodynamics of melting of polymer crystals' was summarized in two basic papers on defect polymer crystals. These papers were finally published in England despite many objections from referees who did not grasp the importance of non-equilibrium processes [33]. A path of 'zero-entropy-production melting' using fast heating was proposed, in opposition to the generally accepted slow heating. The rationale was to achieve a quick transition from the metastable crystal to the equally metastable melt. Slow heating, in contrast, brings changes in perfection of the crystals and may suggest erroneously high melting points. For random copolymers, slow melting has some use in detecting the last crystals which dissolve into the concentration which is set by the synthesis and unaffected by segregation caused by the crystallization.

The other metastable state, the glass, was also analyzed in our laboratory. A special, sequential heating and cooling method was invented, a method called ‘dynamic differential thermal analysis’ or DDTA [34]. The kinetics of the freezing of polystyrene was derived mathematically [35] and compared to the DDTA experiments, using the hole model of the liquid-state, as applied to polymers by Hirai and Eyring [36]. It could be demonstrated that the glass transition temperature T_g changes logarithmically with cooling rate, and that the hysteresis (enthalpy relaxation) can be described mathematically. The rather cumbersome equations could be solved with the help of an electronic computer. Studying all of the available calorimetric data on the change of the heat capacity, C_p, at T_g allowed us to formulate ‘the rule of constant increase of C_p per mobile bead within a molecule at the glass transition temperature’ [37]. This rule states that ‘every flexible part of a molecule (bead), has a heat capacity increase of about 11 J (K mol of beads)’. It permits the estimation of the flexibility of a molecule by thermal analysis, and also documents that the change in heat capacity at the glass transition temperature is an extensive thermodynamic quantity and can be used to find the amount of amorphous material in a multi-phase material.

Besides metastable states, the equilibrium state is always in need to be well characterized since it forms the limit against which the metastable state must be assessed. Heat capacities are the basis of all thermal properties and are in this characterization most important. The total heat content, H, is not measurable directly. It must be measured by summation of all the incremental amounts of heat capacity [$C_p=(dH/dT)_{p,n}$, heat added per kelvin at constant pressure, p, and composition, n]:

$$H(T)=H(T_0)+\int_{T_0}^{T} C_p \mathrm{d}T \qquad (1)$$

This equation underscores the importance of either to measure heat capacity over the whole temperature range, or to develop a theory that allows extrapolation of incomplete data. This latter approach was taken in our laboratory for the evaluation of the heat capacity of solids (glasses and crystals).

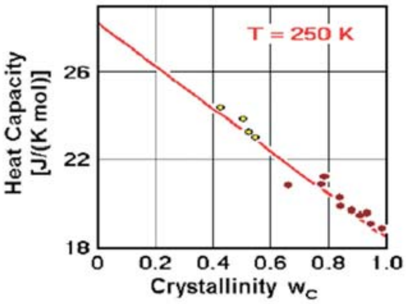

Fig. 2 Extrapolation of the measured C_p to the crystalline and glassy PE. Filled circles refer to linear PE, open circles to branched

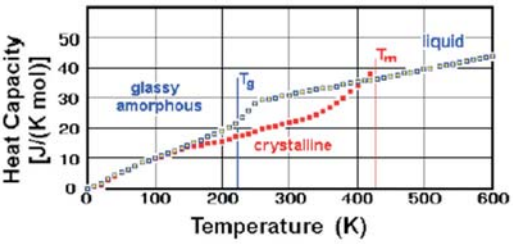

Fig. 3 Heat capacity limits for liquid and crystalline PE as can be gained from extrapolation of data as shown in Fig. 2. Note the broad glass transition

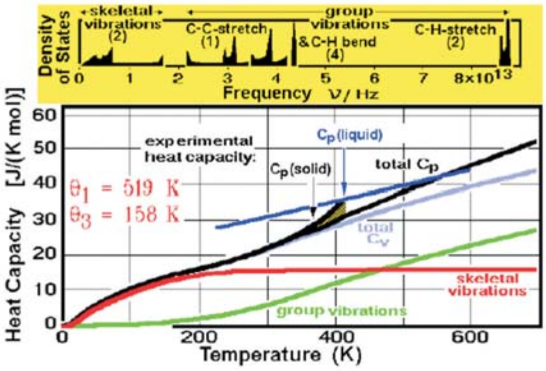

Fig. 4 Contributions to the heat capacity of polyethylene

In the solid-state the heat capacity is caused almost entirely by vibrational energy. Based on the work by Einstein [16], Debye [17] and Tarasov [18], an approximate vibrational spectrum was fitted by us to the heat capacities that are often only known over a limited temperature range. Polyethylene (PE) was the first fully analyzed sample [38]. The experimental heat capacities [26] were combined with all literature values to a data-set that could be extrapolated to 100% crystallinity, as shown in Fig. 2. The limiting extrapolated heat capacities are given in Fig. 3. The fit to the approximate frequency spectrum consisting of skeletal and group vibrations is shown in its later, final form in Fig. 4 [39]. For the first time, the measured equilibrium thermal properties could be linked to a vibrational spectrum to understand the motion in the solid-state of high polymers [40]. It was then also possible to give quantitative information for the crystals on the degree of order, via the entropy S, and the stability, via the free enthalpy G. Figure 5 displays the final result. This first analysis has led over the years to similar analyses of over 200 polymers and polymer-related materials of low molar mass.

Figure 3 displays also the heat capacity of the amorphous state (crystallinity=0%). At high temperature this is the melt, at low temperature the glass. The

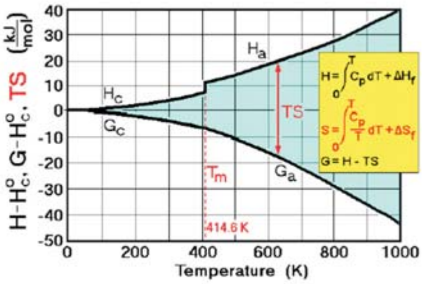

Fig. 5 Thermal properties of polyethylene: enthalpy, *H*, free enthalpy, *G*, and entropy *S* (as *TS*). The subscripts are: *a* for amorphous and *c* for crystal. The link to the experimental heat capacities is established by the equations in the insert

glassy state is quite difficult to reach for the fast crystallizing polyethylene, but Fig. 3 displays clearly the glass transition temperature of 237 K. Of special interest is also the rather gradual beginning of the glass transition, starting at about 120 K. This was explained as a slow beginning of local conformational motion (*gauche-trans* equilibrium) on the basis of estimates of the energy and by interpretation of mechanical properties and NMR data [41].

These first ten years of research in polymer morphology and thermal properties confirmed the value of full analyses of materials using structure and energy considerations. It became clear that the two roots of the full description of materials are their mass and energy. Quantitative methods for the measurement of mass and energy were equally well developed at the beginning of modern science, some 200 years ago [42]. Based on the constancy of combining ratios of the masses of elements in chemical reactions, Dalton [43] could prove the atomic theory of matter. This started the development that today lets us ‘see’ molecules in full structural detail. The magnification factor to go from the atomic scale (0.1 nm or 1 Å) to the macroscopically visible scale (1 μm) is 10^4. While the research into the mass of matter took now a path to find more and more structural detail on an atomic, microscopic level, the research into the energetics went in the direction of a macroscopic description through thermodynamics [44]. Its link to molecular motion was limited largely to the description of ideal gasses ($pV=nRT=1/3M\bar{v}^2$ where $\bar{v}^2$ is the mean square particle velocity). The reason for this preference of macromolecular description of the energetics is the even larger scaling factor needed to ‘visualize’ molecular motion in the condensed states. This feat became only possible more recently through simulation of crystals on supercomputers [45]. The molecular time scale for large-amplitude motion is in the picosecond range (10^{-12} s). Compared to the fastest directly observable processes that take perhaps one millisecond (10^{-3} s), one needs a scaling factor of 10^{-9}! This is much further removed from human experience than the structure information. The understanding of the link of molecular motion to thermal and mechanical properties is only now developing rapidly.

First DSC and morphology (1965–1975)

The availability of commercial DSC equipment that was far superior to any self-built instruments falls into the beginning of this time period. We bought our first Perkin-Elmer DSC-1 in 1965 and repeated within a few days measurements on the by then available completely crystalline and extended chain crystals of polyethylene [46] to extend the earlier effort on semicrystalline polyethylene discussed in ‘Early calorimetry and knowledge about solid polymers (1955–1965)’. The quality of the new data rivaled even those gained by adiabatic calorimetry [26]. Coupled with dilatometry, the equilibrium melting temperature T_m^0 could be fixed within a fraction of a kelvin to be 414.6 K and the difference between equilibrium and non-equilibrium dissolution temperatures could be used to estimate the surface free energy γ (0.083 J m^{-2}) using the Thomson–Gibbs equation [47]:

$$\Delta T = \frac{2\gamma T_m^0}{\Delta h_f \rho l} \qquad (2)$$

where Δh_f is the heat of fusion (293 J g^{-1}), ρ, the density (1.0 Mg m^{-3}), and l the lamellar thickness. A lamella of 10 nm thickness has a specific surface area of 200 m^2 g^{-1} and leads to a ΔT of 23.5 K. The enormous surface areas of polymer crystals explain most of their metastability. This straight-forward experimentation revealed two additional important facts. First, the heat capacity of polyethylene is what one would expect from extrapolation of paraffin data. Later research detailed that the continuous change in C_p with chain length is due to a steady increase in skeletal vibration frequencies, starting with solid hexane [48]. Second, extended-chain crystals melt rather slowly and can lead to ‘superheating of polymer crystals’, i.e., melting is slower than the conduction of the heat of fusion into the sample [49]. A new field of study was initiated, the ‘kinetics of melting’, to be contrasted to the kinetics of crystallization. This topic was also our contribution to the First and Second International Congresses on Thermal Analysis at Aberdeen, Scotland and Worcester, MA in 1965 and 1968, respectively (ICTA) [50]. In Aberdeen, our contribution was one of only five in the field of polymer science (131 papers, overall). Things have changed over the years, polymer science is by now the main contributor to thermal analysis, chiefly due to the easy availability of DSC and its capability of high precision.

The about 100 publications that were generated from 1965 to 1975 at RPI can be summarized in six major topics that are discussed next with key citations: 1) The work on 'extended-chain crystals' was continued [51]. 2) It led to the study of 'crystallization during polymerization' [52]. 3) This, in turn, led to the discovery of 'molecular nucleation' [53]. 4) A number of polymers besides polyethylene were analyzed. 5) The glass transition of pressure-densified polymers was measured. 6) A major effort was made to write-up completed subjects as books or book chapters [11, 21, 54] and a new teaching method that of the Audio Courses was experimented with [55]. All throughout, thermal analysis was providing the direction for new research and basis of better information on materials.

The knowledge gained on extended-chain crystals [51] was the key for the understanding of metastability in polymer crystals, polyethylene being the model for all flexible macromolecules. We originally thought seeding with equilibrium crystals might help in growing more stable crystals, but it just did not work [56]. Thermal analysis showed that there is only little enhancement of crystallization due to the presence of this most perfect crystal substrate. It was also shown in this research that folded chain crystals are initially less perfect and anneal subsequently at the crystallization temperature to a more perfect state [56]. Towards the completion of crystallization, lower-melting crystals form. These observations suggest limits of the classical theory of polymer crystal growth which is based on single-step addition of segments that span the full lamellar thickness [21, Vol. 2]. Morphological details of the nucleation, growth, annealing, and melting were generated by electron microscopy [57, 58]. The distribution of the observed nuclei excluded the commonly assumed utility of secondary nucleation in crystal growth. Obvious locations of secondary nuclei were ignored by the molecules on crystallization. Experiments on polypropylene and computer simulations led Binsbergen to quite similar conclusions [59]. Secondary nucleation does not seem to govern the crystallization rate.

The mechanism of chain extension on crystallization of polyethylene under elevated pressure provided another puzzle. From the microcopy of the crystals and the thermal analysis of melting it was clear that the initial crystal had to be chain folded [51]. The chain extension had to be a subsequent annealing step [58]. Why, however, does the more restrictive crystallization under high pressure permit chain extension? This question was resolved in two stages. First, Bassett observed in 1972 that at elevated pressures, a hexagonal phase is stable [60]. The corresponding phase diagram is shown in Fig. 6. We could later identify this hexagonal phase as conformationally disordered, as a 'condis crystal' [61]. Only condis crystals have the required high mobility for fast diffusion of the chains through the crystal for full chain extension. Although not all flexible polymers that crystallize as condis phase anneal to extended chain crystals, all the extended-chain crystals grown from the polymer melt are condis crystals [62]. Pressure, in turn, is not a prerequisite. Examples, of extended chain crystals which can grow at atmospheric pressure are poly(tetrafluoroethylene), poly(chlorotrifluoroethylene), poly(diethylsiloxane) and *trans*-1,4-polybutadiene.

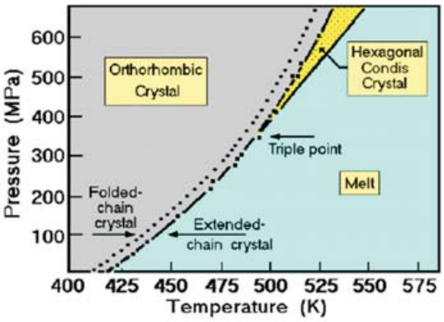

Fig. 6 Phase diagram of polyethylene

Having observed initial chain folding even for extended-chain crystals, I felt certain that one can formulate a 'chain-folding principle' [21, Vol. I, p. 193]: 'A sufficiently regular, flexible linear macromolecule crystallized from the mobile, random state will always crystallize first in a chain-folded macroconformation'. This chain-folding principle has naturally a corollary. It should be possible to grow extended chain crystals directly on 'crystallization during polymerization', bypassing the polymeric, random state. My first sabbatical leave 1966/67 at the University of Mainz was used to investigate this question [52]. Many indications that extended chain crystals of polymers can grow from the monomer were already in the literature, and a series of examples were analyzed by us in the following years (selenium from the vapor [51, VII and IX], poly(oxymethylene) from trioxane [63], polyparaxylylene from the cyclic paraxylylene dimer [64], polyethylene from diazomethane [65], lithium polyphosphate from the lithium dihydrogen phosphate [1] and poly(tetrafluoroethylene) from the gaseous fluoroethylene [51, VIII]. For more details see also [21, Vol. 2]. Figure 7 shows the schematic of extended chain crystal growth of poly(oxymethylene) inside a single crystal of trioxane. Similar simple mechanisms can often lead to fully extended equilibrium crystals of flexible macromolecules. A large number of intermediate cases have also been identified where crystallization occurs shortly after polymerization. In these cases the degree of chain folding is an indicator of the separation of polymerization and

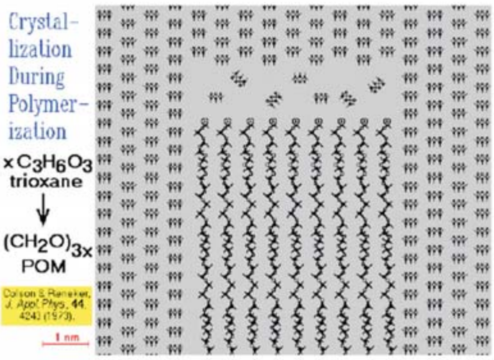

Fig. 7 Schematic of crystallization of poly(oxymethylene) during polymerization from trioxane crystals

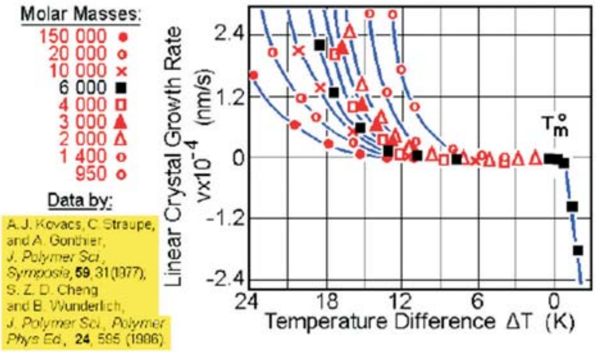

Fig. 8 Illustration of the break between crystallization and melting rates for poly(oxyethylene)s of different molar mass

crystallization in location and time. This turned out to be specially important for the discussion of biological syntheses, as in celluloses and silks, as examples [21, 52]. The crystallization during polymerization provides also the bridge to the knowledge of crystallization of small molecules.

It was suggested above that secondary nucleation was not the rate-determining step in crystallization of flexible polymers. If it is not, what takes its place? The crystallization kinetics of all analyzed flexible polymers had shown an exponential crystallization rate, dependent on the inverse of the supercooling, a clear sign of some type of nucleation control [21]. This seeming contradiction is not yet fully resolved, but a qualitative discussion can be given as follows: Plots of melting and crystallization rates *vs.* temperature exhibit breaks, as shown in Fig. 8. The kinetics is not continuous through the equilibrium melting temperature, in contrast to the Onsager's principle of microscopic reversibility. There is a region of metastability below the equilibrium melting temperature where the melt is metastable. Even seeding with stable crystals does not break this metastability [56]. Our study of crystallization indicated, in addition, that a growing crystal in a melt of a broad distribution of molar masses can reject with perfect selectivity molecules of sizes that are sufficient to lead to stable crystals [66]. Such segregation must have a reversible step. Our suggestion is that there must be a 'molecular nucleation' step [53, 67]. The molecular nucleus involves, depending on supercooling, all or a portion of every molecule as the first step of crystallization. The molecular nucleation provides the rate-limiting step [21]. This proposal maintains the proper rate dependence of crystal growth (Fig. 8), explains the molecular mass segregation and satisfies the reversibility of crystallization/melting, but now on a single-molecule level. Once a molecular nucleus exists, melting and crystallization are reversible on the molecular scale. If the molecule is completely removed from the crystal surface, new molecular nucleation with the necessary supercooling is required, explaining the break in Fig. 8. Although a quantitative description of molecular nucleation is still outstanding, all of the many experimental results observed seem to be in qualitative agreement with the molecular nucleation concept. Besides the model polyethylene [53, 66] an even more complete analysis was carried out later on poly(oxyethylene) [68].

The detailed thermal analysis beyond polyethylene began with poly(oxymethylene) [63]. Superheating, double and triple melting peaks, crystal perfection on heating, recrystallization, annealing and ultimately decomposition could be observed. General free enthalpy diagrams were derived that permit to visualize the metastable states and their transitions, as shown in Fig. 9. All the indicated transitions could be documented and their special signature in thermal analysis was identified. Other polymers studied included poly(ethylene terephthalate), of interest because of its ease of change of the backbone structure

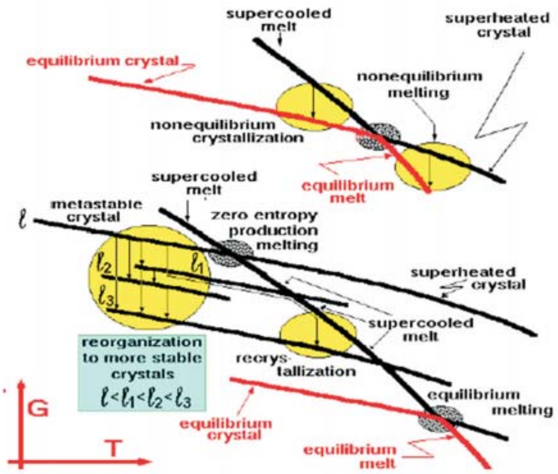

Fig. 9 Free enthalpy diagram to correlate the various equilibrium and non-equilibrium states of polymer crystals: annealing, reorganization, recrystallization, crystallization and melting. Upward transitions between the states are forbidden by the second law (ΔG must be negative or zero)

through etching and solid-state polymerization [69]; selenium, a polymer that can open its folds to anneal to extended chain crystals [70]; polyparaxylylene, that shows several polymorphs and can be crystallized during or immediately after crystallization [71]; polycaprolactam (nylon 6) that can also be polymerized into the solid-state [72] and poly(tetrafluoroethylene), a molecule with an intriguing polymorphism [73]. Another set of compounds that caught our interest were tetraalkyl ammonium salts [74]. More will have to be said later about these compounds and their mesophases.

The work on glass transitions was continued with a study of the hysteresis for glucose, selenium, poly(vinyl chloride), polystyrene, poly(methyl methacrylate), and poly(oxy-2,6-dimethyl-1,4-phenylene) (PPO) [75]. The parameters for the kinetic description [35] were determined. As expected, low- and high-molar-mass compounds behaved similarly. What was not expected was that densified glasses obtained on vitrification under elevated pressure did not have a lower enthalpy. On annealing they showed a relaxation with different relaxation times for dilatometry and calorimetry [76]. This precludes a description of the glass transition as solely free-volume- or entropy-governed processes, as frequently done to reach a simple description. Between parts of molecules residing in different crystals are ties which form the bridges between crystalline and amorphous phases, first suggested by electron microscopy [21]. Their presence could be proven by DSC followed by selective dissolution [77].

This large volume of new information needed to be fit into an overall picture. A second sabbatical was spent entirely in the library at RPI to complete a treatise on macromolecular physics [21]. The flexible macromolecules were placed into a general ‘system for classifying molecules’, as shown in Fig. 10. Another clarification introduced was the nomenclature for the shape as a whole for flexible macromolecules: the ‘macroconformation’. The term macroconformation is distinct from the term conformation which describes the limited arrangement about one or several bonds (also called rotational isomerism) and the term morphology which describes the shape of the crystal. The limiting macroconformations of polymers are identified in Fig. 11.

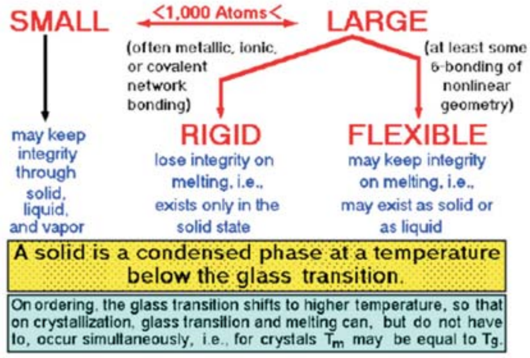

Fig. 10 Summary of all types of molecules

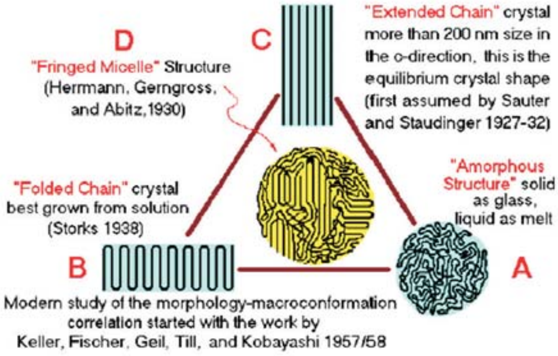

Fig. 11 Molecular macroconformations that describe the shape of polymer molecules within crystals, melt and glasses

The summary of the emerging knowledge about defects of polymers as described in [21, Vol. 2] led to the introduction of the idea of ‘amorphous defects’. An amorphous defect is a three-dimensional defect, caused by molecules that are partially included in the crystal. It is thus a phase, but of nanometer size. Initially amorphous defects were assessed only by crystallinity, but they must be tied intimately to the crystal, since the bulk-amorphous phase does crystallize, the amorphous defects do not. Together with the chain folds, they are the major causes of metastability in the polymer crystals. Later research built on these initial observations.

Increasingly troublesome proved that the object of my specialization, polymer science and thermal analysis, could not draw enough students within most universities to justify a full-time teaching effort. This does not mean that I did not enjoy the freshman chemistry teaching, but I felt that the unique knowledge that was accumulated over the years of research could not be taught in proportion to its potential value to science and industry. An experiment was made with developing of audio courses [55]. Special, condensed lectures were recorded for the audio courses and combined with books of summaries and blackboard material. Each of the courses was equivalent to one semester, 3 credit hours. Although not the same as live lectures, the audio courses provided detailed instruction to anyone interested, independent of teaching schedules and location, and of particular value to the increasing number of graduate students with English as the second language. At RPI, the Evening Division handled the student registration, and I arranged for up to six hours of personal tutoring, exams, and grading through oral exams. The courses ran cost effective. Indeed, it would have been possible to reduce the tuition from the high private-school level and still be profitable. More than 200 students went through these audio courses at various locations. It opened the possibility for a professor to teach simultaneously at several universities and companies. The local organization would provide the students interested in the subject, schedule occasional personal visits by the author, and if needed, run tutorials and schedule exams. The experiments showed that the method works, but universities (and professors) are still too conservative to underwrite such changes in teaching methods with their wide-ranging implications.

Computerization and formal development of ATHAS (1975–1988)

The time period of this section brought a special advance in thermal analysis. Computers were added to DSC for data acquisition, treatment, and ultimately for analysis and storage in a form to give easy access at a later time (data banks). In our laboratory the modification began with adding electronic calculators with a tape or card punch for mass data storage [78]. Next, we found that expert help from computer programmers was necessary to design a fast computer that could do both acquisition and calculation of data [79]. Later, the manufacturers introduced their own, proprietary software. This latter development may have hampered independent programmers to create the specialized, more transparent software that is needed for many scientific applications. In a workshop at the 8th ICTA in Bratislava this problem was discussed and suggestions were made, but largely ignored by all manufacturers of DSCs [80]. Today it is still not easy to link the DSC output directly to data banks, thermodynamic function generators and independently developed or acquired mathematics packages.

The introduction of affordable personal computers of the Apple, Comodore and Atari trade marks at about 1980 did not only provide entertainment with games. These personal computers were also ideally suited to produce sound and pictures for instruction in thermal analysis in the form of computer courses [81]. All that was needed was 32 kB of RAM. For about 20 years, these programs ran on the old computer in our laboratory. They included lectures, exercises, and exams. Modern computers are dominated by the not so teaching-friendly Microsoft programming, so that more recent teaching with computer courses comes only now to fruition, but still lacks the original voice capability. It is discussed in ‘Molecular motion and disorder (1988–1996)’.

The research during this time period at RPI is documented in about 140 publications and centered around the idea of generating better thermal analysis and making fullest use of the emerging computer capabilities. This summary starts with a description of the ‘Advanced THermal Analysis System’ (ATHAS) in Fig. 12, and treats the analyses of new glassy and crystalline polymers. It ends with a major effort to understand mesophases.

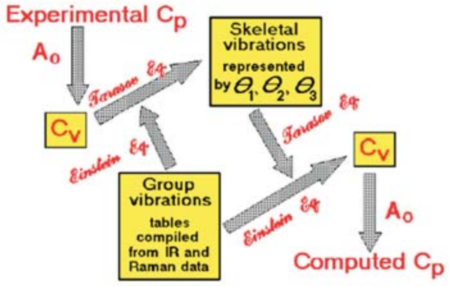

Fig. 12 The ATHAS, developed for the computation of heat capacities of crystals and glasses of macromolecules

The idea of ATHAS is rather simple. It is based on the knowledge gained with the early analysis of the heat capacity of polyethylene as detailed in ‘Early calorimetry and knowledge about solid polymers (1955–1965)’. To extend the initial effort to other polymers, we created a critically reviewed data bank of experimental heat capacities [82]. All data in the literature were uniformly presented in data tables, compared to parallel measurements and judged for precision. This data bank is since 2001 under the direction of M. Pyda and available over the internet [83]. Having just an archival data bank was, however, not our goal. The data bank was to be the base for further advances. Figure 12 illustrates the scheme followed for the analysis of the heat capacity of solids that are expected to have mainly vibrational contributions to the heat capacity. First the C_p needs to be changed to C_v. Since the thermodynamic relationship:

$$C_p = C_v + TV\alpha^2/\gamma \tag{3}$$

requires information on expansivity α and compressibility γ, quantities that are often not available for a given polymer, we adapted the Nernst–Lindemann equation to polymers as:

$$C_p - C_v = 3RA_0 C_p T / T_m^0 \tag{4}$$

where A_0 can either be fitted to limited experimental α and data γ, or taken as a universal constant of $3.9\cdot10^3$ K mol J^{-1} [84]. The next step was the computation of the heat capacity contribution of the group vibrations using information based on infrared and Raman spectra. The calculation involves mainly Einstein functions [16] and combinations of one-dimensional Debye functions [17]. Subtraction of this contribution from C_v yields the experimental skeletal heat capacity. The inversion of the skeletal heat capacity gives the parameters of the Tarasov function, Θ_3 and

Θ_1 [18]. The computation programs and a discussion of the results are given in [85]. The value of Θ_3 represents approximately the upper frequency limit of the intermolecular vibrations, and Θ_1, the upper limit of the intramolecular chain vibrations. This analysis accounts for the left half of Fig. 12. By carrying out the computations in reverse, as indicated by the right half of the figure, C_p due to the vibrations in the solid can be calculated at any temperature. Figure 4 shows the results of such a computation. Starting at about 250 K an increasing deviation from the vibrational heat capacity occurs. It could later be linked by molecular dynamics simulation to defects in the crystal ('Molecular motion and disorder (1988–1996)'). Analyses for more than 100 polymers are now available in the ATHAS Data Bank [83]. Starting with 1981, a biannual ATHAS Report was issued, describing the progress in thermal analysis. The eighth report of 1995 concluded this series. Further information becomes available as soon as it happens by listing on the internet, a practice that is to be continued from the University of Rzeszow by Dr. Pyda.

The theoretical description of heat capacities of liquids was attempted based on statistical mechanics approximations, but did not lead to simple analyses [86]. Liquid polymers and solid polymers with insufficient experimental data, as well as copolymers and blends are better analyzed using empirical addition schemes based on group contributions [87]. Overall, heat capacities are with these methods predictable to 3–5% precision. Once the analysis is completed, the integral thermodynamic properties can be evaluated, as shown in Fig. 5. The needed transition parameters are usually measured independently and extrapolated to equilibrium. A listing of the presently best available information is also contained in the data bank [83].

The study of glassy polymers involved di- and tri-block copolymers of styrene and α-methyl styrene and a comparison with a blend of the same component composition [88]. A number of noteworthy observations were made. First, in the microphase-separated block copolymers the glass transitions were broadened asymmetrically. The upper end of the glass transition of the polystyrene phase (T_g=373 K) is surrounded by the glassy poly(α-methyl styrene) and is spread to higher temperature, while the beginning of the glass transition of poly(α-methylstyrene) (T_g=441 K), surrounded by polystyrene melt, is shifted to lower temperature. Ultimately, both glass transitions merge and cover the full 68 K between the two glass transitions. The blend of homopolymers of the same two components was compatible at low and incompatible at high molar mass. The glass transition could be used for evaluation of partial or full phase separation. The glass transition of the solution was shifted, as expected, to an intermediate temperature, but it was also broadened symmetrically. This broadening of the glass transition of polymer solutions is an observation that can be made also on polymer solutions with low molar mass solvents. Only if the two components are fully mixed, as in a random copolymer, is the glass transition as sharp as in homopolymers [89]. The symmetric broadening may result from the remaining unmixed neighbors along the chain direction, i.e., homopolymers in solutions remain unmixed in one dimension.

Poly(tetrafluoroethylene), PTFE, is a polymer that crystallizes easily, so it was difficult to observe its glass transition. A search of the literature indicated 36 different T_gs spread over 300 K. Quenching a PTFE copolymerized with a small amount of hexafluoropropylene led to a sample of only 17% crystallinity. With help of the data bank heat capacities, a broad glass transition centering about 200 K could be identified [90]. This was one of the first times the utility of the data bank was made use of. With the limiting heat capacities of both liquid and solid well established, the glass transition can be identified even if it spreads over more than 100 K.

The glass transitions of partially crystalline polymers are of particular interest. An analysis of poly(ethylene terephthalate) and several other polymers showed that the hysteresis observed on slow cooling followed by fast heating did not occur on most of the semicrystalline polymers [91]. In addition, the increase in heat capacity at T_g was often reduced more than expected from the independently measured crystallinity. This means that above the glass transition temperature the heat capacity is less than expected [91]. This observation was quantified on poly(oxymethylene) and the missing melt was called the 'rigid amorphous fraction' (RAF) [92]. The rigid amorphous fraction has later proven to be of great importance in the understanding of mechanical properties. It gives a quantitative measure of a distinct third phase in partially crystalline polymers, and expands on the concept of the nanophase-size 'amorphous defects' [21].

The first sabbatical in this time period was spent by writing Volume 3 of Macromolecular Physics [93], a summary of the knowledge about melting. Also, an extensive review of the basis of thermal analysis was prepared [94], and besides updates of the audio courses [55], a computer based freshman chemistry lecture and workbook [95] were completed. The aim of the latter was to introduce students very early to the applied side of chemistry by teaching the understanding of engineering applications through polymer and solid-state knowledge.

With new insight gained from scholarly work, new observations on the glass transition, and the backing of the growing data bank, many polymers were analyzed from 1975 to 1988 using the ATHAS of Fig. 12. Much more information could be extracted from thermal analysis because of the ability to understand the irreversible transitions as shown in Fig. 9, the knowledge of the equilibrium limit, the quantitative information on C_p due to vibrations only, and the measured or extrapolated liquid C_p. The polymers studied covered a wide range. There was the inorganic polymer selenium [96] with its intriguing chemical reactions that allow chains to rearrange and change into rings and the two-dimensional polymers of the group IV chalcogenides [97] which need to be described with a two-dimensional frequency spectrum. The basic, flexible macromolecules polyethylene [98], poly(ethylene terephthalate) [99], poly(4-methyl-1-pentene) [100], poly(oxyethylene) [101], fluoropolymers [102], and polypropylene [103] were revisited to improve the data bank and to establish transition parameters. A series of more modern, stiffer-chain molecules were analyzed, including polyparaxylylene [104], poly(oxy-1,4-phenylene-oxy-1,4-phenylenecarbonyl-1,4-phenylene) (PEEK) [105], poly(oxy-2,6-dimethyl-1,4-phenylene) (PPO™) [106], poly(ethylene-2,6-naphthalene dicarboxylate) [107], poly(butylene terephthalate) (PBT) [108] and poly(thio-1,4-phenylene) and poly(para-phenylene) [109].

The newest class of polymers of this time period were macromolecular liquid crystals, LCs. Macromolecular LCs were first observed in form of lyotropic*** systems [110] and discussed in terms of segmental rigidity [111]. When thermotropic, polymeric LCs**** which need no solvent were mentioned in the scientific literature [112], it became of interest to find the similarities and differences to small-molecule LCs. Naturally, our data bank was ideally suited to form the basis for a detailed thermal analysis. We started first with a number of thermal analyses and tried to understand the new properties, such as LC glass transitions, heat capacities, and ordering and disordering transitions [113]. This was followed with a review of the subject that led to the discovery that many of the macromolecules classified as LCs belonged actually into a different, new type of mesophase, the ‘conformationally disordered phase’ in short, the ‘condis phase’ [61]. This new phase was obvious when applying the general ‘rules for the entropies of fusion based on molecular shape and flexibility’ which were discovered when researching Volume 3 for the Macromolecular Physics [93]. The rules are listed in Fig. 13 together with ‘a system of classifying phases and mesophases’. The condis phase is closest to the crystalline state since it has neither positional nor orientational disorder of the molecule. The conformations, however, are locally mobile and disordered. They change by jumping between the different rotational isomers. Overall, this leads to the possibility of easier diffusion along the chain direction as needed for chain extension, as discussed in ‘First DSC and morphology (1965–1975)’. The importance of this discovery led me to spend my fourth sabbatical in 1986/87, with the help of a Humboldt Prize, at the Universities of Freiburg and Ulm (Germany). Many discussions and research projects were undertaken to learn the intricacies of the condis phase. The experience of this year is summarized in [61] and a series of papers were published that deal with the differences between the mesophases [114]. On my return from Germany, I was offered a Distinguished Scientist position at UT and ORNL, and chose early retirement from RPI as of Jan. 1, 1988, after almost 25 years of service.

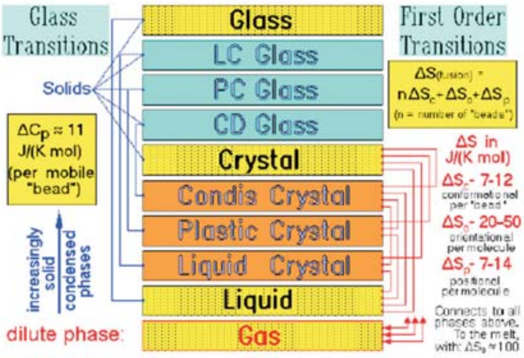

Fig. 13 A summary of phases, their transitions and properties as well as the rules that govern the entropies of transition

Molecular motion and disorder (1988–1996)

It was mentioned in the Introduction that time goes fast. This must be true since it seems like yesterday that we moved ATHAS from RPI to The University of Tennessee and Oak Ridge National Laboratory. With only one student, Mr. Xenopoulos, research was begun from scratch. By 1996, this work was documented in more than 150 papers. The new teaching effort has produced a textbook on thermal analysis [115, 116] and a new, existing method of teaching using text, figures, and hypertext displayed by computer. The latter are available over the internet and

---

*** Lyotropic liquid crystalline phases derive their anisotropy from interactions with solvents.

**** A thermotropic LC has an LC/isotropic phase transition temperature at T_i, in contrast to a lyotropic LC that usually does not lose its structure at higher temperature.

have been continually updated with the last version released in 2006 [117].

Thermal analysis experienced during this period of time a stage of rapid development, brought about by the introduction of faster and more precise calorimetric measurements and data analyses. The measurement of heat capacity by DSC has always been troubled by the need to make a series of three runs: first, a baseline scan of two empty differential calorimeters (empty sample and reference pans), to be followed by a calibration scan (usually with sapphire), and then concluded by the sample run. For critical work this should even be followed by a repeat of the baseline scan to be assured that nothing has changed during the first three runs. The main problem of calorimetry invariably is the difficulty to control heat losses. As an improvement, we developed a single-run instrument based on a commercial triple calorimeter [118]. After initial calibration of the asymmetry of the three-pan positions, a single run could produce good heat capacities.

A much more revolutionary approach was offered by temperature-modulation of the DSC (TMDSC). The sample temperature, T_s, and the temperature difference, ΔT, show in this case a small, sinusoidal variation of frequency ω [119]. Typical modulations of T_s are 0.1 to 1.0 K at 0.1 to 0.01 Hz. In this way any heat loss, occurring most likely with a different frequency, can be eliminated. Figure 14 illustrates the method of modulation and gives a comparison between the two methods. The details of mathematical descriptions and applications are available in the literature [120]. Of importance was the proof that steady state can be achieved even in the presence of modulation when e^{-K_t/C_s} becomes negligible:

$$T_s(t) - T_0 = q\left[t - \frac{C_s}{K}(1 - e^{-K_t/C_s})\right] + \tag{5}$$
$$+A_{T_s}(\cos\varepsilon\sin\omega t - \sin\varepsilon\cos\omega t + \sin\varepsilon e^{-K_t/C_s})$$

where $T_s(t)$ is the time-dependent sample temperature, T_0, the starting temperature, q, the underlying, constant heating rate, C_s, the C_p of the sample calorimeter (pan+sample), K is the thermal conductivity constant, and ε is the phase shift relative to the block temperature, expressed by:

$$\sin\varepsilon = \frac{\omega}{\sqrt{\left(\frac{K}{C_s}\right)^2 + \omega^2}} \tag{6}$$

The heat capacity can then be extracted from the maximum amplitudes A of the modulation, as set for the sample temperature T_s, and measured for the temperature difference ΔT:

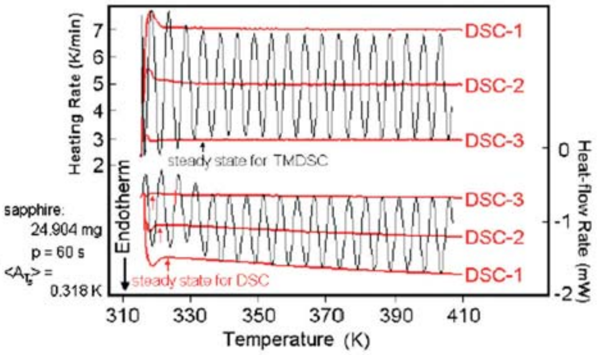

Fig. 14 A comparison of DSC and TMDSC. (For details see [120], as well as 'Reversible melting and the rigid-amorphous phase (1996–2003)', below [158])

$$(C_s - C_r) = \frac{A_{\Delta T}}{A_{T_s}}\sqrt{\left(\frac{K}{\omega}\right)^2 + C_r^2} \tag{7}$$

where C_r is the heat capacity of the reference calorimeter (empty pan). Besides measurement of heat capacity, it is also possible to distinguish between thermal processes that occur equally on heating and cooling (such as C_p), and others, that do not (such as the latent heats during crystallization/melting). The temperature modulation of the DSC, thus, is an important new technique for the study of the many irreversible processes in polymeric materials [120].

The prior research period closed with the discovery of the importance of conformational motion and disorder in polymers. Such increase in disorder is measured by an increase in entropy beyond that given by the vibrational heat capacity. Examples are the beginning of devitrification (Fig. 3), the introduction of defects below the melting temperature (Fig. 4), and the transitions to mesophases such as liquid crystals and condis crystals (Fig. 13).

A research program on molecular dynamics simulations of crystals was developed in cooperation with Dr. Noid of ORNL. His programming skills allowed to simulate motion of up to 30000 atoms for as long as 10^{-10} s by integrating the equations of motion from a chosen initial state. The results are described in about 35 joint publications. Over the years the simulations took almost 8000 h of supercomputer time. Overviews are given in [45], and Fig. 15 demonstrates the information of importance to thermal analysis. In the upper left of Fig. 15, one can see the skeletal vibrations within a crystal as snapshots of segments of seven neighboring chains. The upper right plot shows the increasing concentration of *gauche*-bonds that can be counted in a crystal that should ideally have only *trans*-rotational isomers. The change of a *trans*-conformation to a *gauche*-conformation is the basic large-amplitude motion of flexible polymer backbones. The beginning of a sizeable concentration agrees with the in-

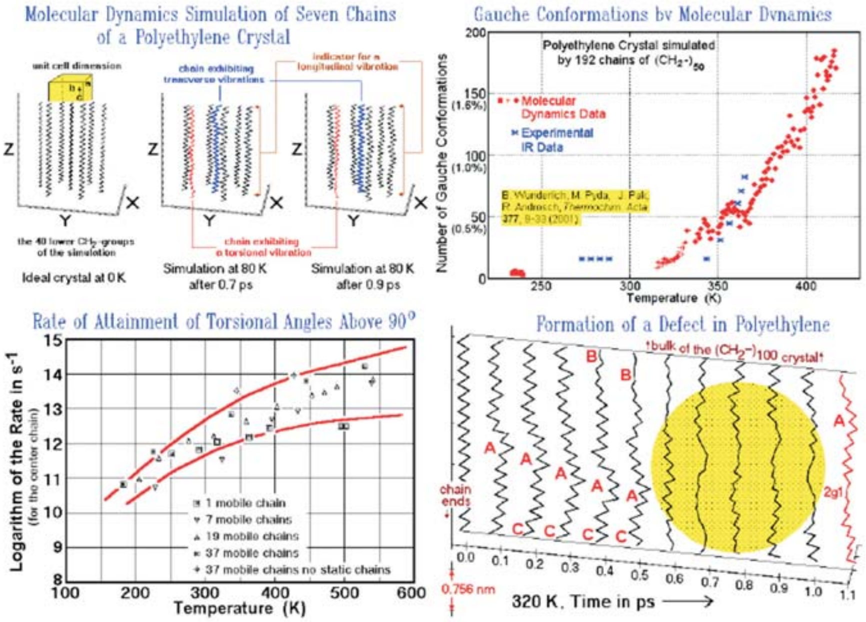

Fig. 15 Molecular dynamics simulations showing skeletal vibrations, concentration of *gauche*-conformations, rate of formation of *gauche*-bonds, and the mechanism of kink formation (A, B and C indicate the tramsverse, torsional, and longitudinal vibrations of the upper left of the figure)

crease in heat capacity seen in Fig. 4. The same increase in heat capacity was also found for all paraffins [48] and other polymers that have long paraffinic chain segments. Despite the relatively low *gauche*-concentration at anyone time, the rate of *gauche*-bond formation per bond is enormous, as shown in the lower left of Fig. 15. The curves apply to different simulation conditions using 1 to 37 chains of $(CH_2-)_{100}$ enclosed in rings of static chains (constant volume simulation) or without static rings (constant, zero-pressure simulation). The corollary of low concentration and fast rate of formation is a lifetime in the picosecond range. Combinations of two *gauche* defects lead to a kink, the long proposed more stable point defect in polymer crystals [121]. With the help of kinks, crystal deformation can be understood better [45, 122]. The lower right drawing in Fig. 15 illustrates kink formation inside a crystal as a function of time. One can see the collision of all types of skeletal vibrations that provide the energy of defect formation. Based on such simulations, it is possible to visualize for the first time the thermal motion in crystals on a molecular scale. An overall discussion of the defect solid-state of polymers became thus possible, based on experiments and molecular dynamics simulations.

To support the molecular dynamics simulations, thermal analysis is the ideal macroscopic tool. To gain experience and avoid complication of excessive irreversibility known to exist in polymers, we analyzed a series of symmetric tetra-*n*-alkyl ammonium salts, known from past work to be rich in defects [74]. The calorimetry was also supported by microscopic information from ^{13}C solid-state NMR to get direct experimental information on the mobility of specific atoms, and by X-ray diffraction for structure analysis [123]. Combining these results with earlier work [114] it was possible to find the signature properties of plastic crystals, liquid crystals, and condis crystals [124] (also Fig. 13). A number of macromolecules that are located at the border between condis crystals and main-chain liquid crystals could then be identified making use of their phase structure, heat capacity, and large-amplitude mobility [125]. It was interesting to note that in many of the polymeric and small molecules which show mesophases, some of the disordering occurs outside of the transition region. Recognizing such gain of conformational disorder outside of the transition region infers that simple analyses using baseline separation of the heat capacity leads in these cases to substantial underestimations of the heats of transition.

For a long time we hesitated to study polymeric fibers by thermal analysis because of their complex structure. The observation that crystals in highly drawn fibers could persist far above equilibrium [126, 127] was explained by the strain transmitted from the crystals to the amorphous defects (via tie molecules, also Fig. 9). With the discovery of the rigid amorphous phase [91, 92] it became clear that on drawing of fibers the rigid amorphous phase had to change its structure to 'oriented, intermediate phases'. With two oriented and one amorphous phase, the number of possible phase structures increases considerably, as shown in Fig. 16. Only the phases on

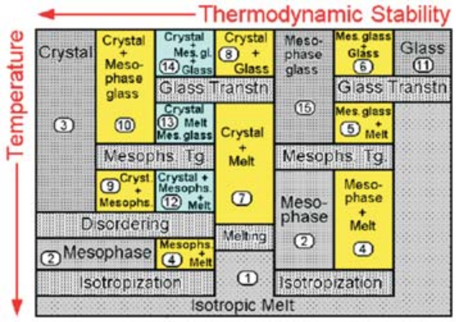

Fig. 16 Phase diagram of a three-phase system with metastable states. The equilibrium states are found on the left side, transitions are indicated by the densely dotted boxes, the numbers indicate the 15 possible phase areas

the left side are in equilibrium. All others may appear as metastable states. Size, orientation, shape, structure, mobility and interfaces of the phases need to be considered for the understanding of the basic structure-property-processing triangle.

Our work was helped by the X-ray expertise of Dr. W. Busing of ORNL. He taught us how to make a full-pattern Rietvelt analysis of the fiber diagram of, for example, poly(ethylene terephthalate) [128]. Figure 17 shows clear structural evidence of a substantial amount of an oriented, intermediate phase. Its amount and orientation are proportional to fiber modulus and tenacity. The crystallinity and the perfection of crystals are of secondary importance [128]. Another fiber that has been similarly analyzed is gelspun ultra-high molar mass polyethylene [129]. In this case almost all polymer chains are parallel to the fiber direction, but not all participate in the crystal. By solid-state ^{13}C NMR we could show that the not crystallized *trans*-chains had a much higher mobility, although less than the small amount of remaining amorphous material. Both examples documented the interrelationship of structure and mobility which is the basis of thermal analysis.

The work on the completion and computerization of the ATHAS Data Bank accelerated at UT and ORNL with the possibility to employ more permanent coworkers [82]. Thermal analysis of aliphatic polyamides (nylons) [130] indicated a major increase in mobility and disorder of methylene sequences in the crystals before melting [131]. Quasi-elastic neutron scattering confirmed an almost liquid-like conformational mobility within the crystal [132]. A new direction grew out of the research about the polyamides when it was observed that the known heat capacities of a few poly(amino acids) (nylon 2) did not fit into the series of homologs [130]. The problem was resolved by re-measuring not only the few available data, but establishing information for all homo-

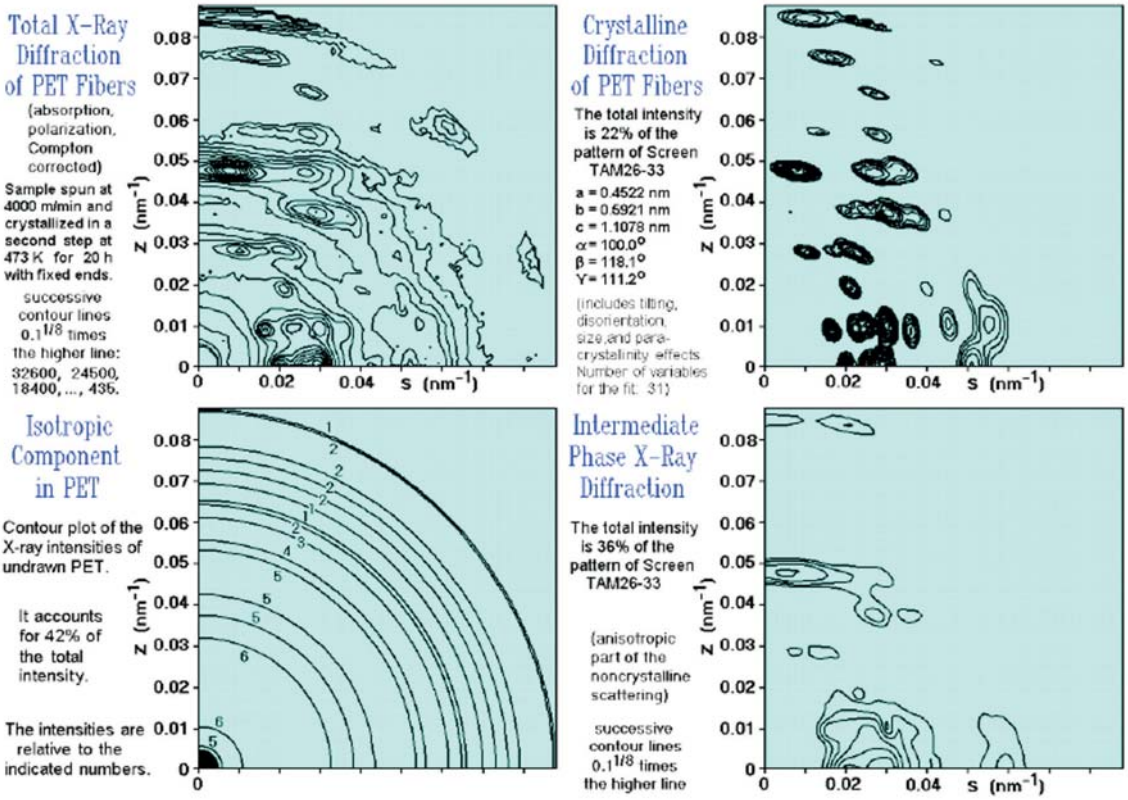

Fig. 17 Rietvelt analysis of poly(ethylene terephthalate) fibers. The X-ray diffraction pattern in the upper left arises from the superposition of the three partial patterns. (Three-phase structure)

poly(amino acid)s and some copoly(amino acid)s that can be made of the 20 naturally occurring amino acids [133]. It turned out that at room temperature and above, all prior measurements had up to 50% errors due to slow evaporation of water. As soon as this groundwork with poly(amino acid)s was laid, we turned to solid proteins. The first step was to find whether the ATHAS method shown in Fig. 12 is also applicable to complicated biological materials. The proof is given in Fig. 18. The root-mean-square errors of the heat capacity due to the skeletal vibrations of a protein are shown to possess a clear minimum for unique values of Θ_1 and Θ_3 of the Tarasov equation [134]. This observation opens the doors for thermal analyses of proteins and allows a discussion of their stability (*G*), disorder (*S*) and enthalpy (*H*), as shown for polyethylene in Fig. 5.

A series of topics that may show greater importance in the future closes out this section. To get to at the root of the problems of thermal analysis, all aspects of phase structure, morphology and molecular motion must be combined with the macroscopic thermodynamics. For crystals of polymers this means to start with an equilibrium single crystal as a base for judging defect structures. This is possible for polyethylene [135] and some crystals grown during polymerization [21, Vol. 2]. Even more challenging is the effort to make single-molecule single-crystals [136]. The first crystals made proved still metastable, but perhaps it may be possible to anneal them to equilibrium shapes. It may also be of value to see the changes when going to two or three molecules per crystal and to study how the molecular domains can fit within the confines of crystal morphology. Direct observations of atoms is now possible by the method of atomic force microscopy (AFM). We bought an early AFM and could, indeed, 'see' a large amount of atomic and molecular detail [137]. There is hope that this tool for nanotechnology may permit in the future to check on mechanical properties, and why not perform thermal analysis on a nanometer scale? This effort has made large progress in the last 10 years, as will be shown in the next two sections.

Also, new materials are constantly being produced. A very exciting group of compounds are the fullerenes. Shortly after these became available, we analyzed C_{60} [138] and C_{70} [139]. As one would expect, plastic crystal phases with beginning motion outside the transition region could be quantified by the ATHAS analysis. At room temperature these highly symmetric fullerenes rotate freely in the crystalline state that is stable up to very high temperatures. The large spaces in the crystal between the touching molecules can hold small molecules like toluene with almost chemical-bond-like stability and hinder their mobility. Again, thermal analysis and solid-state NMR were the tools that could resolve this behavior by quantitative interpretation of the transitions and increases in heat capacity outside the transitions.

Thermal analysis has progressed far in linking microscopic causes to the observed macroscopic observations. Whenever such a link is well understood, predictions of the properties of new or proposed materials can be made. Sometimes, these predictions are good enough to almost obviate the need for further experimentation. This leaves, however, the areas that are not supported by a well-worked-out theory. In this case it is still possible to make predictions by using neural net calculations. The first attempts at neural net predictions in the field of thermal analysis showed great promise [140].

Reversible melting and the rigid-amorphous phase (1996–2003)

This second period of research at UT and ORNL was perhaps the most productive in my professional carrier. The close cooperation with senior members of the Polymer Group of ORNL added breadth and needed

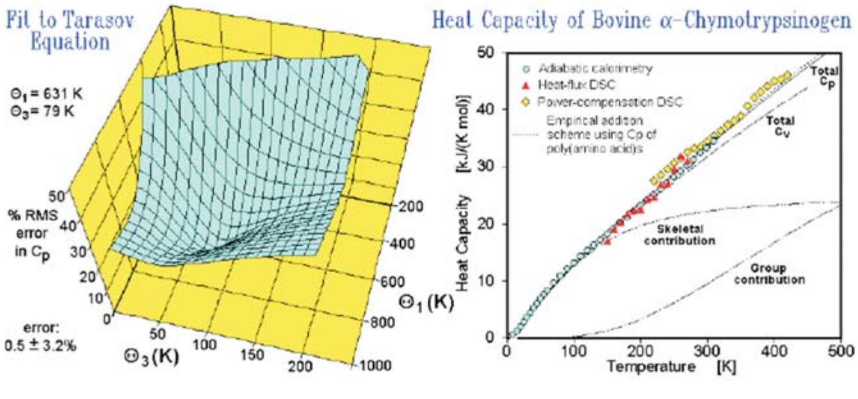

Fig. 18 Minimization of the error for the description of the skeletal heat capacity of a protein. Bovine α-chymotrypsinogen of type II, 245 amino acid repeating units with a molar mass of 25646 Da and 3005 skeletal vibrations [134]. The right graph is a comparison of calculation and measurement

Fig. 19 Polymer Research Group from UT and ORNL. Front row, L to R: Dr. M. Varma-Nair, Dr. K. Roles, Dr. B. Wunderlich, Ms. J. Hikson (Secretary) Dr. A. H. Narten (Leader of the ORNL Polymer Group), Mrs. C. Sumpter. Middle, R to L: Dr. B. G. Sumpter, Dr. A. Xenopoulos, Dr. J. Cheng, Dr. A. Habenschuss (ORNL), Dr. L. Liang, Dr. W. R. Busing (ORNL). Top three, L to R: Dr. D. W. Noid (ORNL), Dr. B. K. Annis (ORNL) and Dr. Y. Jin

expertise to the effort to understand polymers. The result can be seen in the joint publications described in ‘Molecular motion and disorder (1988–1996)’ and the present ‘Reversible melting and the rigid-amorphous phase (1996–2003)’ and ‘Decoupling of chain segments of flexible macromolecules (2003–)’. Figure 19 is a picture of the researchers from UT and ORNL in the early 1990s. Our central theme was the probing of the amorphous, crystalline and mesophase structures of different molecular mobility on the macroscopic (thermodynamic) and microscopic (atomic) level, as indicated in the classifications in Figs 10, 13 and 16, summarized for thermal analysis in [141, 142]. The development of the tools was described in ‘Molecular motion and disorder (1988–1996)’, consisting, besides the basic calorimetry and TMDSC, of computation, X-ray diffraction, solid-state NMR and varying types of microscopy. In these eight years, about 180 publications were completed and much was added to the picture of solid polymers beyond the state described some 50 years ago [20]. Two specific reviews tie the work in our laboratory to the general literature. The first dealt with the newly emerging field of soft-matter nanophase physics [143], the second, with the major results derived from quantitative TMDSC by testing for local reversibility and properties of different nanophases [144]. In these two articles, the knowledge generated in 350 publications from many laboratories was combined to the picture of semicrystalline polymers as ‘globally metastable and multi-phase structure with subsystems of micro- and nanometer size’. The latter subsystems may even show local reversibility and are ‘coupled’ by the large molecules which frequently cross the phase boundaries. (See also the recent treatise [116] and the learning tools [117, 145]).

In this ‘Reversible melting and the rigid-amorphous phase (1996–2003)’, it will be shown in five steps that (a), the new instrumentation of TMDSC and the mastery of temperature modulation and data deconvolution has increased the precision of heat capacity. Application of experience from reversible heat capacities and its separation from the irreversible latent-heat effects, then, permits to better understand (b) glass transitions and (c) first order transitions. In many cases a new ‘intermediate phase’ is needed for the description. One of these intermediate phases is (d), the rigid amorphous phase [91, 92] which often is a nanophase and may also be partially oriented and then shows a latent heat on disordering. In the final paragraph (e), the expansion of the continuing work on new polymers for the data bank into biological macromolecules and precisely structured copolymers are described. The latter lead in ‘Decoupling of chain segments of flexible macromolecules (2003–)’ to the important concept of decoupling of molecular chain segments. Finally, research into making single-molecule single-crystals, and to use microcalorimetry on very small samples are mentioned. These efforts to find direct calorimetric information on small and metastable systems suggests the use of fast measurements [103]. This is the prime progress predicted for the 21st century [146]. The progress on superfast calorimetry is also described in ‘Decoupling of chain segments of flexible macromolecules (2003–)’.

(a) Instrumentation of TMDSC matured during this second research period at UT and ORNL, 5–10 years after first use of temperature modulation [119]. A first problem was the asymmetry of the twin calorimeters which is corrected in standard DSC with the difference in heat flow rates of a run with two empty pans. This proved more difficult to correct in TMDSC. The phase-shift of the reversing heat-flow rate in the time domain loses its sign (±) on Fourier transformation into the frequency domain when calculating the amplitude of the reversing heat flow rate [147]. A preliminary solution was to assure an asymmetry of known positive or negative value. By now, calorimeters with asymmetry correction are available based on modeling using an electrical-analog circuit (Q 1000 MDSC of TA Instrument Inc., Tzero software®) [148].

A similar computation was fitted in our laboratory to the Mettler-Toledo DSC, as shown in Fig. 20 [149]. The strong frequency dependence of the heat capacity below periods of about 100 s for typical commercial instrumentation can be corrected for, as seen from the center curve of the figure. Turning in Fig. 21 to a third DSC available in our laboratory, it is illustrated how a saw-tooth modulation of the sample temperature allows even multiple frequencies to be analyzed simultaneously by Fourier transform of the heat flow rate response [150]. The Fourier components are seen in the upper left insert. Using the five harmonics indicated, and four different sawtooth periods, the shown 20 data points could be generated. Analyzing the data by applying Eq. (7) with an empirical function τ instead of C_r/K yields a frequency dependence of the heat capacity as shown in the lower left insert. The low frequency dependence is linear, as expected from Eq. (7) (see inner insert), but at ω^2=0.5 (a period of about 4.5 s), deviations start, but τ remains a continuous function of frequency and can be calibrated, so that the reversing heat capacity is simply:

$$mc_p = \frac{A_{HF}}{A_{T_s}\omega}\sqrt{1+[\tau(m)]^2\omega^2} \qquad (8)$$

with τ being a function of sample mass and frequency. Since different samples also give different values of τ, different calibrations apply to the sapphire calibration run and the measurement. The thermal analysis with sawtooth modulation has also been analyzed with the standard DSC method, by separately investigating the linear heating and cooling segments and comparison with an overall Fourier-transform into the various harmonics [151]. In this case direct information about the irreversible process can be obtained, which otherwise is available only indirectly from the difference between total and reversing responses. A more complex sawtooth was created with close-to equal amplitudes of the different harmonics by linking of 14 linear heating and cooling segments [152]. This complex sawtooth can be generated in any standard DSC which permits to link and repeat the different segments. With these methods, measurements of heat capacity which approached ±0.1% were possible,

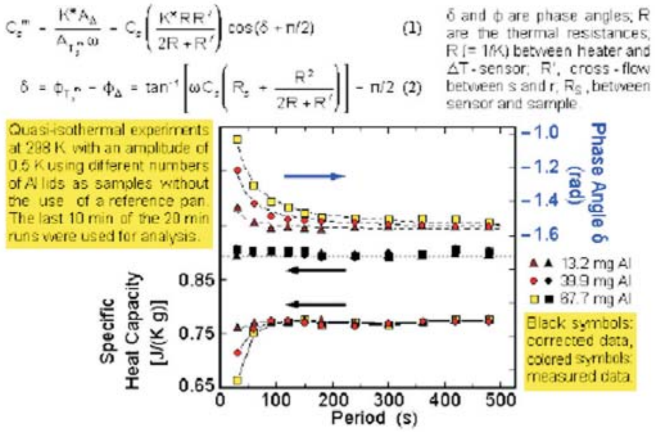

$$C_s^m = \frac{K^* A_\Delta}{A_{T_s^m}\omega} - C_s\left(\frac{K^* R R'}{2R+R'}\right)\cos(\delta+\pi/2) \qquad (1)$$

$$\delta = \phi_{T_s^m} - \phi_\Delta = \tan^{-1}\left[\omega C_s\left(R_s + \frac{R^2}{2R+R'}\right)\right] - \pi/2 \qquad (2)$$

δ and ϕ are phase angles; R are the thermal resistances; R (= 1/K) between heater and ΔT-sensor; R', cross-flow between s and r; R_S, between sensor and sample

Quasi-isothermal experiments at 298 K with an amplitude of 0.5 K using different numbers of Al lids as samples without the use of a reference pan. The last 10 min of the 20 min runs were used for analysis.

Black symbols: corrected data, colored symbols: measured data

Fig. 20 Measurement with a Mettler-Toledo TMDSC of type 821 as a function of frequency ω (=2π/period). The measured heat capacity is C_s^m, A indicates the amplitudes of sample temperature, T_s, and the temperature-difference response is Δ. The value of C_s is the (known) heat capacity of Al, and K^* is the calibration constant which fits the vertical offset of the heat capacity, found by analogous measurements with sapphire

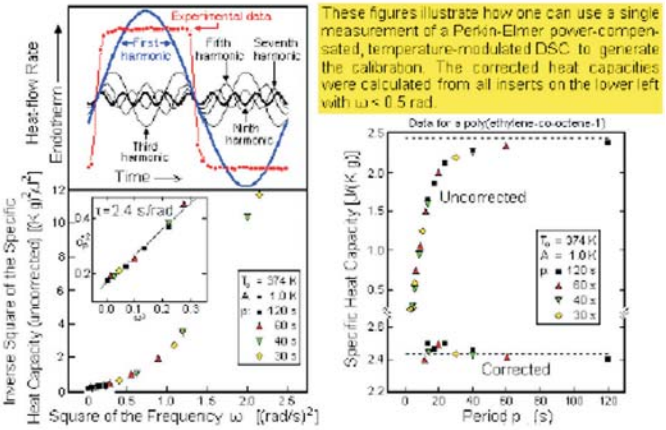

These figures illustrate how one can use a single measurement of a Perkin-Elmer power-compensated, temperature-modulated DSC to generate the calibration. The corrected heat capacities were calculated from all inserts on the lower left with ω < 0.5 rad.

Fig. 21 Measurement with a Perkin-Elmer TMDSC of type 7 as a function of frequency ω (=2π/period). The measured specific heat capacity can be corrected with Eq. (8) using a τ which above a period of about 4.5 s is dependent on sample, sample mass and also frequency. The value of τ is given by the slope of the curves in the lower left diagram approaching the precision of classical adiabatic calorimetry [153].

All data for high-precision heat capacity determinations were generated with quasi-isothermal measurements which consist of a modulation about a constant base temperature for 20 min or longer with the first few modulation cycles discarded, to avoid the initial approach to a steady state seen in Fig. 14. This method is of particular importance for samples which change their phase structure during the measurement and absorb or generate irreversible latent heats. The quasi-isothermal measurement, then, can be extended until the irreversible processes cease. The TMDSC with an underlying heating rate, however, is also capable to produce heat capacity data in the absence of such slow irreversible changes [154].

The temperature gradients within the calorimeter were studied by direct, contact-less, infrared thermography [155] and faster modulation by infrared light, using a pulse-width modulation to create multiple-frequency measurements. In the latter experiments we used standard DSC equipment to detect the calorimetric response [156]. Detailed modeling of TMDSC [157] allowed to collect enough experience to tackle the data interpretation when large amounts of latent heat are present to destroy linearity and stationarity of the measurement, as well as to discuss the usefulness of the introduction of a complex heat capacity [158, 159]. Figure 22 is an example of the simulation of the reversing heat flow rate *HF*(*t*) on sharp melting, followed by similarly sharp crystallization. As indicated, the total heat flow rate <A_{HF}> and its smoothed value are largely different from the expected value. This is caused by the loss of stationarity of the sliding average <A_{HF}> which must be changing close to linearly to allow the deconvolution of the reversing *HF*(*t*) from the total [160].

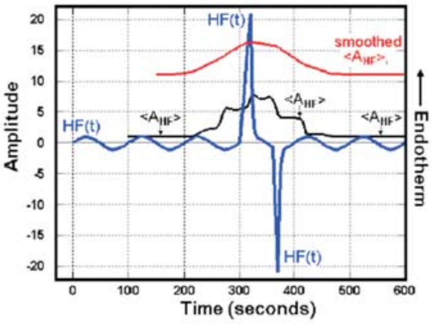

Fig. 22 Simulation of a single (equilibrium) melting and crystallization. The heat flow rate averaged over sliding period of modulation is <A_{HF}>. It is not equal to the standard DSC result because of the missing stationarity on deconvolution

(b) The first detailed study of time-dependent heat capacity concerned the glass transitions of poly(ethylene terephthalate) of different degrees of crystallinity and amorphous polystyrene [161]. Figure 23 illustrates the approximate separation of the non-reversing and reversing heat capacities, and the extrapolation of the experimental data to a larger range of frequencies. Note that the non-reversing heat capacity represents the difference between the total

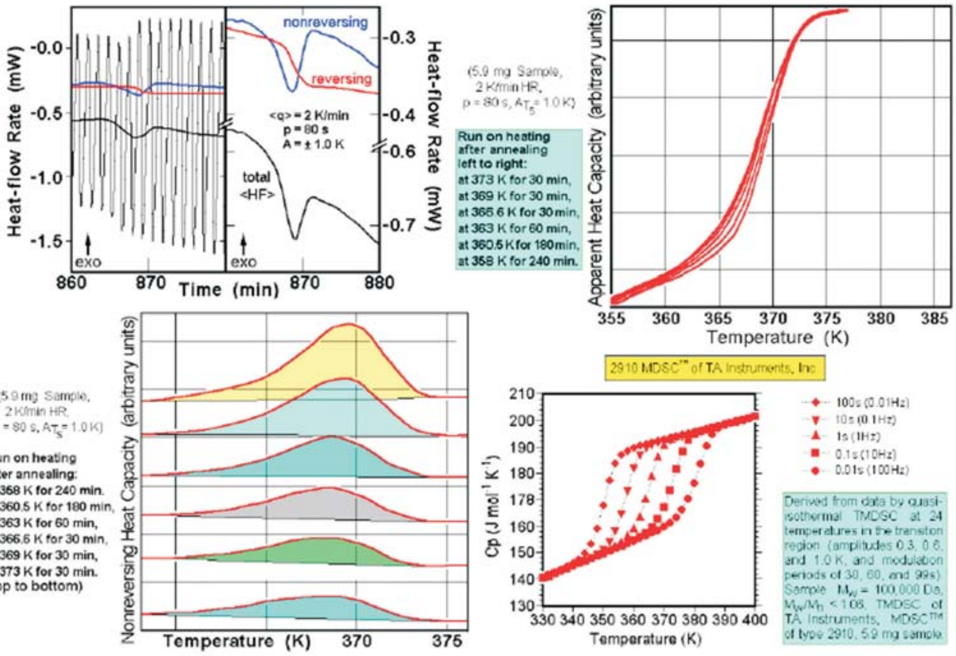

Fig. 23 Temperature-modulated DSC of polystyrene. Upper left: Raw raw data of the heat-flow rate, total, reversing and non-reversing. Upper right, reversing C_p showing differences for the different thermal histories. Lower left non-reversing C_p, illustrating the hysteresis. Lower right: frequency dependent C_p

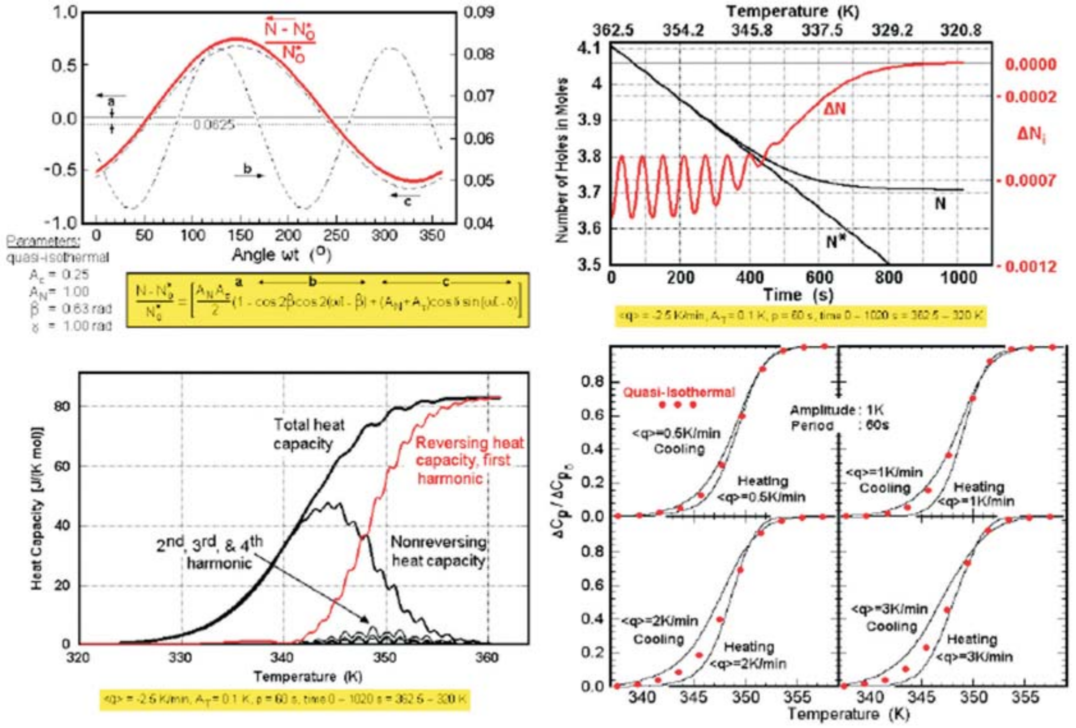

$$\frac{N-N_0^*}{N_0^*}=\left[\frac{A_N A_E}{2}(1-\cos 2\beta\cos 2(\omega t-\beta))+(A_N+A_T)\cos\delta\sin(\omega t-\delta)\right]$$

Fig. 24 Computations from TMDSC data of poly(ethylene terephthalate) using a simple hole theory. Upper left: the three different, normalized contributions to the number of holes (*N* is the instantaneous hole concentration, *N** the equilibrium, β and γ are phase angles, *A* denotes constants available from the kinetics). Upper right: changes in *N* during a cooling experiment. Lower left: heat capacities on cooling. Lower right: differences between cooling, heating, and quasi-isothermal experiments. (Only the upper portion of each curve, where the system is close to equilibrium, is in agreement with the calculations.)

heat capacity, measured as the sliding average over one modulation period, C_p(total)=<mc_p>, and the reversing part, mc_p of Eq. (8), which is calculated from the first harmonic of the response of the TMDSC to the modulation of the sample temperature. This procedure approximately separates the heat capacity from the hysteresis effect due to the thermal history. Furthermore, by experiments at different periods, a relaxation time can be assessed and the extrapolation at the bottom right can be carried out.

The data for poly(ethylene terephthalate) (PET) where similarly analyzed, and Fig. 24 illustrates pertinent analyses when assuming that, at least for a small temperature interval, a simple hole theory can describe the glass transition by a hole theory [162] as proposed by Eyring and Hirai [36] and applied already earlier to the glass transition of polystyrene by using a first-order kinetics for the change in concentration of holes [35]. The holes are assumed to be the cause of the observed kinetic phenomena governing viscosity and the change in heat capacity at the glass transition temperature (seen top right of Fig. 24). The top left part of Fig. 24 illustrates that the response of this model to a quasi-isothermal modulation of the sample temperature is only approximately sinusoidal in its change in hole concentration, *N*. There are two small reversible contributions, one (a) being constant and one (b) of double the modulation frequency, in addition to the major contribution (c) of frequency ω. The first harmonic evaluated from the experiment (upper and lower right of Fig. 23) can be compared only to *c* and a suitable theory has to be developed to find the true reversing contribution given by the red curve. As long as this is not done, the calculated non-reversing contribution is in error. A further discrepancy is revealed in the lower left curves for TMDSC with an underlying cooling rate. The constant cooling rate and the modulation show a Doppler-like effect, the frequency on the reversing signal is changing in response to the changing kinetics in the glass transition region. As a result, higher harmonics appear in the Fourier analysis, and the calculated parts of the heat capacity show a remaining modulation which is not observed in the experiments because of an additional smoothing of the data (as indicated in Fig. 22). Finally, the bottom right curves of Fig. 24 illustrates that quasi-isothermal and TMDSC data with underlying heating and cooling rates do not agree, except for the limit of low rates <*q*>. Trying to match the discrepancy with the hole-theory calculations is only successful in the high-temperature portion where the system is close to the equilibrium liquid. This indicates, as the earlier analyses by DDTA [34], that a cooperative model has to be developed to properly model the glass transition. Efforts in this direction have not been successful to date, an estimate of the error, however, can be made, by looking at Figs 23 and 24 (upper right and lower left, respectively).

Further analyses broadened the investigation to semicrystalline samples of different degree of crystallinity, annealing, and orientation. Again, poly(ethylene terephthalate) is an ideal example because its glass transition region is sufficiently lower in temperature than melting, so that for the initial analysis there is no overlap between the transition regions. Figure 25 shows the results from quasi-isothermal TMDSC. The selected curves on the left can also be used to evaluate the time dependence of the amorphous PET, as discussed with Fig. 24. The right plot shows the mathematical representation of the considerable broadening of the glass transition caused by crystallization and ordering, and narrowing by annealing. The final observation is a much larger decrease in the change of heat capacity at the glass transition with crystallization than expected, the signature of the presence of a rigid amorphous fraction, RAF [91, 92].

This comprehensive study of the glass transition [161] makes a connection to the prior analyzed effects of interface, pressure, and mixing effects on homopolymers, polymer solutions, copolymers and block copolymers [35, 37, 75, 76, 88–90]. The correlation of samples on the right of Fig. 25 shows the remarkable decrease in activation energy with crystallization and ordering, which, however, is compensated by a decrease in pre-exponential factors since the glass transitions of all samples begin at the same temperature, as seen in the left curves. In the case of PET and many other polymers of more rigid molecules the RAF goes through a separate glass transition at higher temperature, as will be described below in (d). Observations like this suggest that in such cases the 'RAF' is a separate nanophase, while the broadening of the glass transition of the 'mobile-amorphous phase' is caused by a stress transfer across the interface by incomplete decoupling of the molecules or by freezing-in of local order.

(c) New observations about melting of macromolecules resulted from TMDSC, the tool to probe for reversibility [144]. Quantitative TMDSC was possible after learning how to overcome the experimental problems described with Figs 20–22. First, it was necessary to identify the limits of reversible melting as seen in small molecules like indium [163] and paraffins [164]. Figure 26 summarizes these results. The TMDSC with an underlying heating rate shows that In starts melting as soon as the melting temperature is reached during modulation at point 1 in the upper left figure. The time at or above the melting temperature, however, is not sufficient before the modulation reduces the temperature below the melting temperature and the melted portions of the crystals regrow (exothermic peak 2). This repeats itself until practically all In melts at peak 9 and a small time gap appears before renewed crystallization (peak 10). With the crystallization of peak 16 there is not enough time for crystallization, and after the melting of peak 19 the temperature does not decrease sufficiently for crystallization. The slopes between successive peaks 1–2, 3–4, 16–17 and 18–19, in connection with the temperature profile measured at the pan without contact [155], can be used to discuss the temperature lags within the calorimeter and show that the center of the sample may ultimately develop a melted core of fluctuating size. By reducing the amplitude of modulation and the underlying heating rate, the reversibility of the melting of indium can be bracketed within a few thousands of a kelvin as shown in the quasi-isothermal experiments in the upper right of Fig. 26. Only about 30% of the In

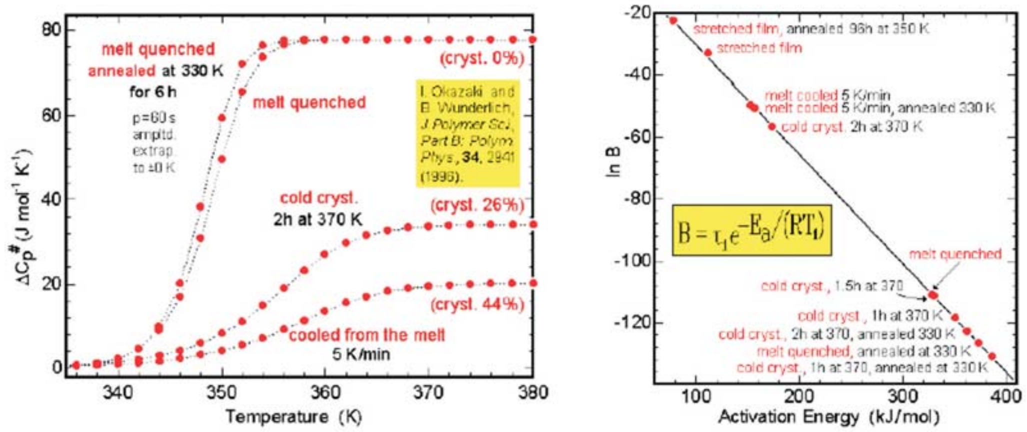

Fig. 25 Apparent reversing heat capacities of poly(ethylene terephthalate) samples of different degrees of crystallinity as measured by quasi-isothermal TMDSC (left), and the correlation of the activation energies and pre-exponential factors (τ_1=132.5 s, T_1=341 K)

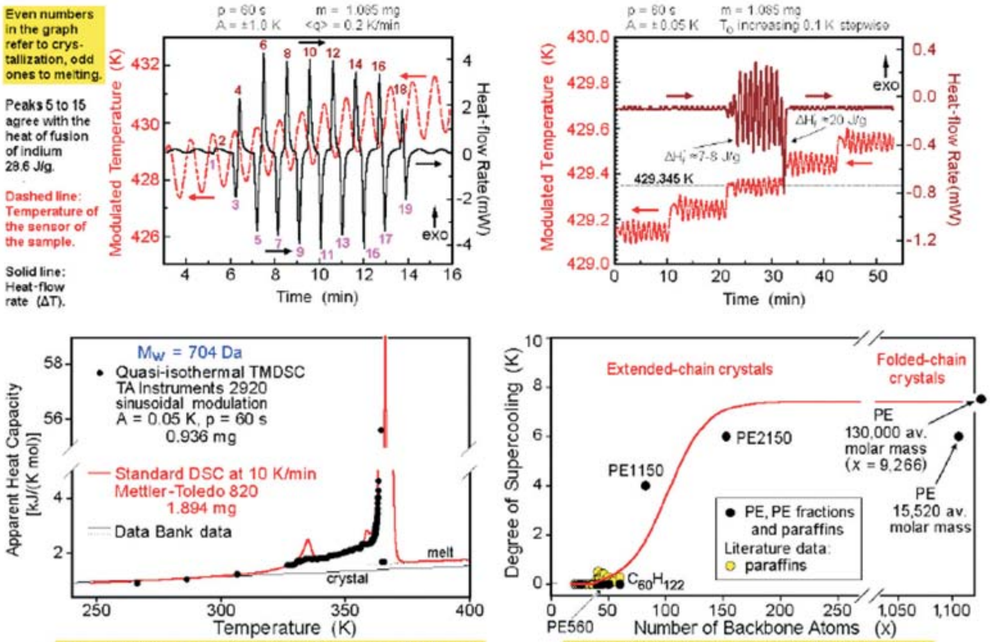
Even numbers in the graph refer to crystallization, odd ones to melting.

Peaks 5 to 15 agree with the heat of fusion of indium 28.6 J/g.

Dashed line: Temperature of the sensor of the sample.

Solid line: Heat-flow rate (ΔT).

J. Pak and B. Wunderlich, *J. Polymer Sci, Part B: Polymer Phys*, **38**, 2810 (2000)

J. Pak and B. Wunderlich, *Macromolecules*, **34**, 4492–4503 (2001)

Fig. 26 Reversible melting, analyzed by TMDSC. Top left: melting of In with an underlying heating rate. Top right: quasi-isothermal TMDSC of In. Bottom left: reversible melting of pentacontane ($C_{50}H_{102}$), comparison of DSC and TMDSC. Bottom right: limits of reversible melting of paraffins and polyethylene

melts at 429.345 K, while none melts higher or crystallizes lower.

Applying this experience with indium to paraffins proves reversible melting of $C_{50}H_{102}$ with the data in the lower left of Fig. 26. The standard DSC beyond the melting peak in the quasi-isothermal runs is caused by instrument lag. As long as the heat-flow rate causing the lag is negligible, DSC and TMDSC yield identical, reversible apparent heat capacities. Similarly, reversible first-order transition peaks could be documented for small and large liquid-crystal molecules [165]. An obvious question arose: How long must the paraffin be to melt irreversibly? This is answered by the bottom right graph of Fig. 26 [166]. At much smaller number of backbone atoms than required for chain-folding, irreversibility is introduced by the need of 'molecular nucleation' (which is in addition to crystal nucleation). Molecular nucleation was already suggested based on crystal growth rates of Fig. 8 and the rejection of lower molar mass species from a crystal of larger molar mass below its equilibrium melting temperature and even zero-entropy-production melting temperature of the correspondingly folded-chain crystal [21, 53, 67].

Although the irreversible melting was easily documented for sufficiently long oligomers of polyethylene, poly(oxyethylenes) (POE), poly(oxytetramethylene) [166, 167], extended-chain crystals of polyethylene (PE) [168], and the crystals of poly(oxy-2,6-dimethyl-1,4-phenylene) (PPO) [169], it was discovered in 1997 that semicrystalline, chain-folded flexible macromolecules like poly(ethylene terephthalate) (PET) [170] and POE [167] must have a 'globally metastable, multi-phase structure with subsystems of micro- and nanometer size', as mentioned in the introduction to this 'Reversible melting and the rigid-amorphous phase (1996–2003)'. Figure 27 illustrates three examples of irreversible melting and one with some reversible melting. Further details about the heat capacity of POE which indicate a 'glass transition of the crystal' will be discussed in (d). The extended-chain sample of PE still has some reversing melting left, due to its broad molar-mass distribution, which however, could be accounted for quantitatively. The PPO also will be further discussed in (d), and the reversing melting of PET is typical as for many other polymers, reviewed in [144]. Other chain-folded crystals which were analyzed in our laboratory relative to their partial reversibility were polyethylene [164, 171] and some of its copolymers [172, 173], poly(trimethylene terephthalate) (PTT) [174], poly(butylene terephthalate (PBT) [175], and polypropylene (PP) [176].

Based on these experiments and the survey of the literature [144], a model for the locally reversing melting was developed and is illustrated in Fig. 28 [177]. This model emphasizes that the reversible melting is mainly concentrating on the growth faces of the crystals. An earlier observed reversible change of the lamellar thickness [178] does not correspond to the close similarity of the reversible and irreversible melting temperatures and has been documented only for polyethylene, while many more polymers show lo-

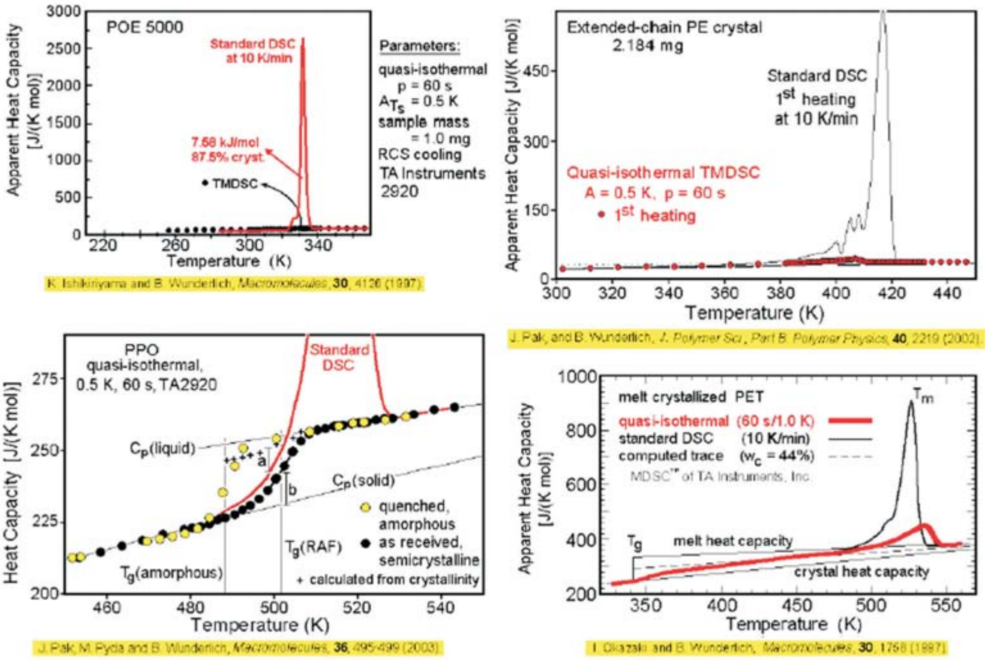

K. Ishikiriyama and B. Wunderlich, *Macromolecules*, **30**, 4126 (1997)

J. Pak and B. Wunderlich, *J. Polymer Sci., Part B, Polymer Physics*, **40**, 2219 (2002)

J. Pak, M. Pyda and B. Wunderlich, *Macromolecules*, **36**, 495-499 (2003)

I. Okazaki and B. Wunderlich, *Macromolecules*, **30**, 1758 (1997)

Fig. 27 Melting polymers by TMDSC. Top left: irreversible melting of extended-chain crystals of POE of molar mass 5000 Da. Top right: irreversible melting of extended-chain PE. Bottom left: irreversible melting and glass transition of PPO. Bottom right: first observation of some reversible melting in PET

cally reversible melting on the growth face, as seen clearly for PP, for example [176]. By comparison with molecular dynamics simulations [45] and the reversible behavior of other polymers [144], this reversible change in thickness was linked to the defect creation within the crystal, seen in Fig. 15, followed by diffusion to the interfaces. The important aspects of the model of Fig. 28 are the 'points of decoupling' which will be shown in 'Decoupling of chain segments of flexible macromolecules (2003–)' to be of rather wide importance to understanding of polymer thermodynamics. For polyethylene, the melting point of decoupled segments can be estimated from the known T_m of folded and extended-chain crystals. The bottom equations on the right of Fig. 28 permits the computation of the melting temperature, $T_{m,2}$, of the extended-chain length of a decoupled segment. The shown curves were calculated by inserting $T_{m,2}$ into the upper equation (instead of 414.2 K, the melting temperature of infinite length) and correcting the melting point lowering (in brackets) for the fraction of the surface covered with chain folds for the given segment length. (For one fold, the correction factor for the term in brackets is 0.50, for two folds, 0.67, for three, 0.75, for four, 0.80 and for five, 0.83.)

An initial attempt to extract kinetic information about irreversible crystallization and melting from TMDSC was made by Toda [179] and was also attempted during this time period in our laboratory with the polyester-imid poly(4,4'-phthaloimidobenzoyl-dodecamethyleneoxycarbonyl) [180]. The method was found to be applicable, but the extracted kinetics is of limited use in arriving at detailed molecular kinetics.

(d) With the basic information about glass and first order transitions (defined by Ehrenfest [181]) as described in (b) and (c), it becomes possible to tackle the much more involved temperature region between the two transitions. In this range of temperature, a frequent overlap of processes is observed, complicating the evaluation of the phase structure and properties. In order to keep within the system of definitions for molecules in Fig. 10 and for phases in Fig. 13, there is still a need to define nanophases. One must go beyond specifying the phase size. It is not sufficient to place the nanophases between the larger microphases, recognized for over 100 years as phases which need their surface properties specified for description, and the loss of validity of the phase concept which occurs at the atomic level of description. To have an operational definition of the nanophase [182], we specified that there should be no bulk phase within the nanophase due to the influence of surface effects throughout the phase [143, 183]. This leaves the actual phase size as a parameter that may be different for each material, but gives a clear distinction of the nanophases from microphases. The typical dimensions of polymeric nanophases are 1–5 nm.

A glass transition broadened to higher temperature does not account for a new phase. One links this effect to the strain transmitted from the crystal. In the center, some bulk-amorphous phase remains. The

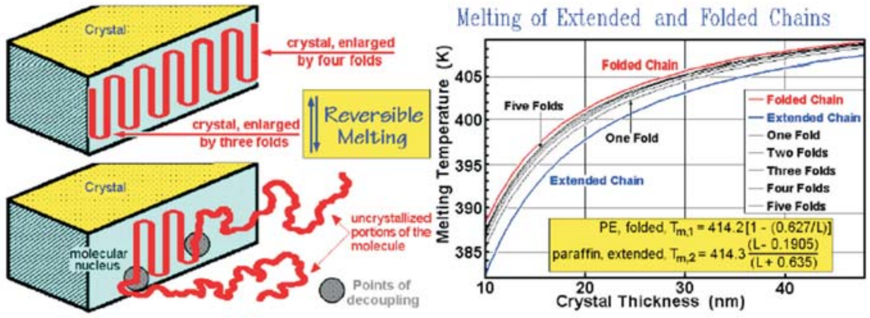

Fig. 28 On the left it is shown how local, reversible melting could occur. The points of decoupling create subsystems on the surface with a lower, reversible melting temperature, as documented on the right

strained layer at the interface could be identified for PE by special electron microscopy [184]. The heat capacity for gel-spun, ultra-high-molar-mass polyethylene is shown in Fig. 29 [185]. The C_p is measured by short-step scanning calorimetry on heating, compared to subsequent cooling scans to check for reversibility. The upper curves show the vibrational heat capacity and the experiment for 100% crystalline PE as in Fig. 4. The fibers A and B are different in degree of annealing (and crystallinity). The actual measured points minus the crystalline heat capacities are shown in the lower graph. They indicate the broadened glass transition which reaches to room temperature, the different levels of amorphous content, and the different beginning of the reversible melting. In addition, the excess of the sum of the amorphous and crystalline phases above 100% suggests that the non-crystalline phase possesses some order, as was earlier discovered as a mobile, oriented, non-crystalline fraction by X-ray diffraction and solid-state NMR [129] and as a result, contributes to the heat of fusion.

A rigid-amorphous fraction, RAF, which does not participate in the glass transition of the bulk phase is seen above in Fig. 25 for PET. It must be a separate phase without any unchanged bulk phase in its interior, i.e., the RAF is separated from the mobile-amorphous fraction. Under the circumstances of its formation, it is likely to be a nanophase. Another example of a polymer with a RAF is PBT, illustrated in Fig. 30 [175]. For the better-crystallized sample on the left, the crystallinity, w_c, of the sample can be calculated from the heat of fusion, obtained by back-integration from above the melting temperature of the apparent heat capacity, subtracting the proper heat capacity. All quantities in the equation of the heat capacity written within the figure, as well as the heat of fusion, must be considered as functions of temperature [4, 26]. This calculation cannot be continued below about 400 K since at lower temperature one can see the separate glass transition of the RAF, with a mid-temperature of about 375 K. The RAF can be evaluated at the upper limit of the broadened glass transition at low-temperature with a mid-temperature of 314 K. Since the lower glass transition corresponds to 42.4% amorphous phase, the difference to the crystallinity yields the RAF of 21.3%. The sample on the right was quenched from the melt. In this case the cold crystallization, reorganization, glass transition of the RAF, and early melting overlap. The standard DSC trace is dominated by the cold crystallization and does not allow any further analysis. From the TMDSC trace, taken with an underlying heating rate, the low-temperature glass transition is obvious, while the glass transition of the RAF is still obliterated by the reversing broad first-order transition. Using, however, the equation for the apparent heat capacity on top of the figure and inserting information about the changes of the RAF in its glass transition from the sample on the left and the change of C_p(liquid) when becoming a glass at the low-temperature glass transition, the complete DSC curves can be approximated. The crystallinity after quenching, thus, could be calculated to be 10%. A remaining unsolved problem for PBT is the origin of the small endotherm below the glass transition which is frequently seen in quenched samples [108, 175].

Clear evidence that below the glass transition the RAF freezes parallel to the isothermal crystallization was brought in the laboratory of Prof. Schick with TMDSC by continuous and simultaneous evaluation of the reversible heat capacity and the total heat flow

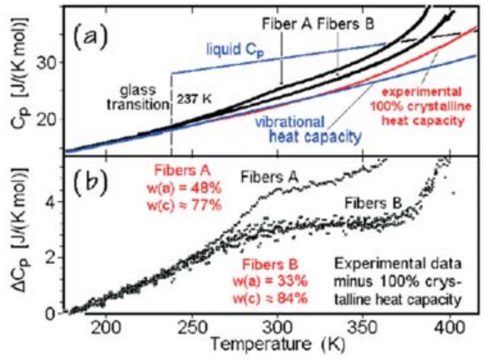

Fig. 29 Heat capacity of gel-spun polyethylene of ultra-high molar mass, compared to the heat capacity derived in Fig. 4

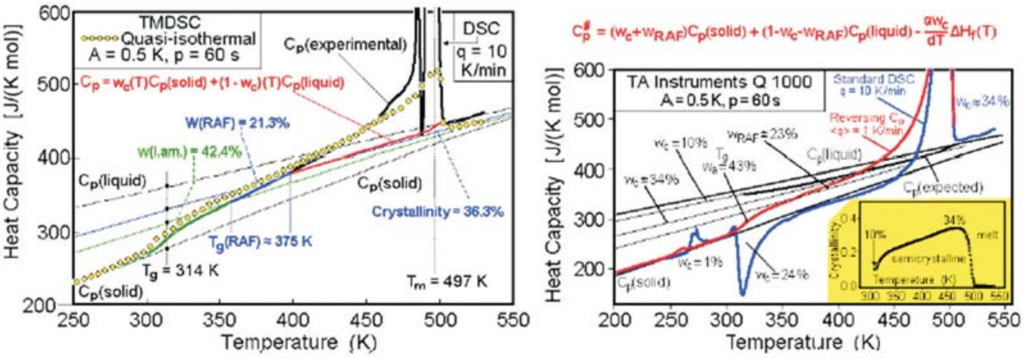

Fig. 30 Standard. DSC and TMDSC of poly(butylene terephthalate) crystallized by cooling from the melt to 36% crystallinity and by quenching from the melt to 10% crystallinity, with a 24% cold crystallization

rate of poly(hydroxy butyrate) for over 55 h [186]. This experiment places the RAF directly adjacent to the crystal and the remaining 'mobile amorphous phase' with a lower glass transition into a separate phase at a different location within the overall metastable structure of the semicrystalline polymer. Returning to the melting behavior of PPO [169], shown in the lower left graph of Fig. 27, it was noted earlier [108] that in this case there was no 'mobile amorphous fraction' below the observed melting peak by standard DSC of the typically 30% crystalline samples (red curve in the figure). The quasi-isothermal TMDSC results prove then that the glass transition of the 70% RAF occurs together with the melting. In fact, by annealing below the melting peak, the crystallinity decreases and the lower glass transition of the quenched amorphous appears [108], indicating that the RAF has actually a glass transition that has moved above the zero-entropy-production melting point so that the RAF keeps the crystals from melting and also prohibits reversible melting. This more detailed behavior of the RAF which could be identified during these years has revealed a quite new picture of semicrystalline polymers. One of the main points is the connection between the crystalline and the amorphous phase which was already observed when analyzing crystal morphology in form of tie molecules and loose loops [21], but has been largely neglected until now. A better understanding and link between mechanical properties and thermal analyses can now be exploited.

(e) Besides the four major research directions in the time period from 1996 to 2003 described in (a) to (d), work continued on the increase of the ATHAS Data Bank [82]. Data were collected for poly(oxy-1,4-benzoyl), poly(oxy-2,6-dimethyl-1,4-phenylene) (PPO), and poly(thio-phenylene) [187]; poly-*p*-dioxanone, poly(trimethylene terephthalate), and poly(butylene terephthalate) [188].

A number of precise copolymers were also analyzed, which turned out of importance in the following research period, described in 'Decoupling of chain segments of flexible macromolecules (2003–)' [189]. Also of importance for this further work was the analysis of such precise copolymer synthesized from large repeating units with respect to their mesophase structure, probed by the crystallization behavior with quantitative thermal analysis, their motional characteristics, measured by solid-state NMR, and their structure by X-ray diffraction [190].

In addition, the effort on thermal analysis of poly(amino acids) and its copolymers and proteins [133, 134], as illustrated in Fig. 18, was brought to a temporary halt after [191, 192] because of a complete disinterest by the appropriate funding agencies. This research was developed exclusively using unrestricted Distinguished Scientist funding, attached to my position at ORNL and UT, and was supplemented by the Polymer Program of NSF as long as the proteins could be justified as plastics. The results showed the beginning of a glass transition in poly(*L*-methionine) and poly(*L*-serine) [192]. From the overall behavior of the proteins, which is similar to the synthetic polymers, one can deduce that there also may be glassy nanophases imbedded in the overall structure, and the local areas of reversible structure-changes could now be quantitatively investigated by TMDSC. The remaining step before linking the poly(amino acid) data [133] to native proteins is the evaluation of the changes of the partial molar thermodynamic functions with changing amounts of water. This step has been spearheaded by Dr. Pyda and is to be continued at the University of Technology in Rzeszow, Poland. Figure 31 illustrates the work on the heat capacity of dry starch. To get quantitative information on the hypothetical heat capacity of liquid 'starch' the prior data on glucose [75] were analyzed as shown on the left, and then used as an estimate on the right. Surprisingly there is a clear beginning of a glass transition in starch at room temperature which, however, reaches only partial mobility. Two additional steps are introduced when water is added to the system.

The updating of the computation scheme for the ATHAS from the main-frame computer to the now

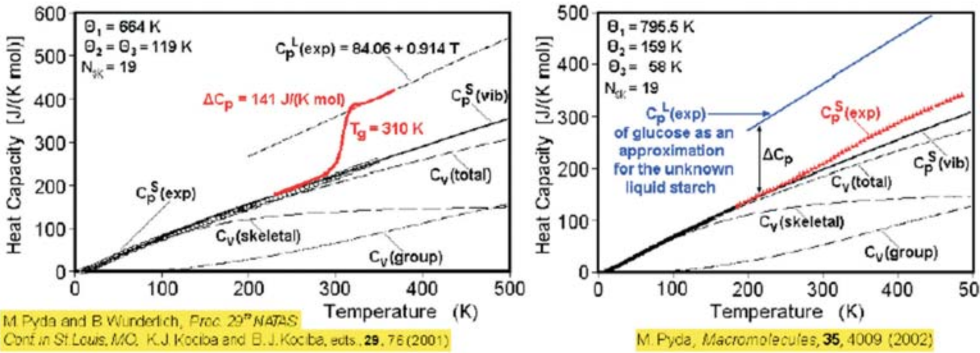

Fig. 31 Analysis of the heat capacity of glucose as model for starch (left), and data on dry starch (right)

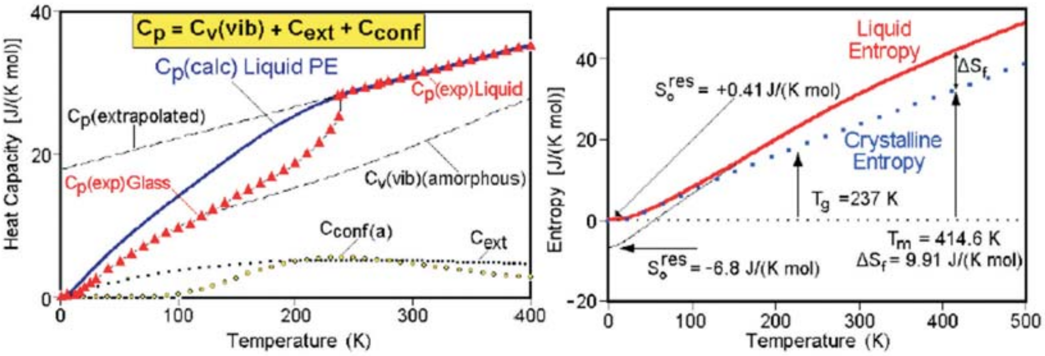

Fig. 32 Calculation of heat capacity and entropy of liquid polyethylene to 0 K without glass transition

sufficiently fast PCs is also listed in [85] and illustrated in Fig. 14. The computation of the heat capacity of liquids has been further developed from the earlier, simple statistical model [86] to an adaption of the Ising model [193] to account to some degree for the cooperativity of the large-amplitude, conformational motion in the liquid. Since these model calculations do not recognize a glass transition at low temperature, it was possible to extrapolate the heat capacity of polyethylene based on experiments (from 250–600 K) to 0 K. Figure 32 shows the results [194]. Using the external contribution, as determined from the liquid expansivity and compressibility, yields still an unreasonable residual entropy of -6.8 J K^{-1} mol^{-1} at 0 K. At the temperature where the conformational contribution reaches zero, the external contribution, however, must similarly reach a value close to zero, as known from the glass. Making this correction, a residual entropy of $+0.41$ J K^{-1} mol^{-1} is reached, and the Kauzmann Paradox [195] is avoided. Note, that the free enthalpy at absolute zero is still large and positive, indicating the metastability of the liquid relative to the crystal. Its value of $+2.1$ kJ mol^{-1} is $\approx$50% of the heat of fusion at the melting temperature [194].

A non-equilibrium phase of poly(4-methyl pentene-1) is shown in Fig. 33 [196]. It was derived from thermal analysis and structure data measured in the laboratory of Prof. Rastogi. Of particular interest is the difference to the phase diagram of polyethylene in Fig. 6. While polyethylene possesses a stable condis phase at elevated temperature and pressure, that of the poly(4-methyl pentene-1) exists only as a metastable phase below the glass transition, similar to polypropylene [103]. The condis glass is reversibly produced by isothermally increasing the pressure at room temperature and reverts on heating to the trigonal phase as shown on the right side of the phase diagram. Also shown is the maximum in the melting temperature which is linked through the Clausius–Clapeyron equation to an inversion of the density difference between crystal and melt. The same inversion occurs on cooling at atmospheric pressure, so that at room temperature the crystal has a lower density than the melt [100].

New X-ray data were also generated for tetraalkyl ammonium salts of small chain length (methyl and ethyl) [197] to support the earlier extensive analyses of the condis-crystal forming salts with up to octadecyl groups [123]. Another small molecule, a neopentane ester, was analyzed with respect to heat capacity, structure, and molecular motion [198]. Finally, the computation of the heat capacities of a series of oligophenylenes was carried out [199], and connected to the earlier calculations and discussions on phenylene-containing polymers [109].

A final topic during this time period dealt with the production and analysis of extremely small samples in

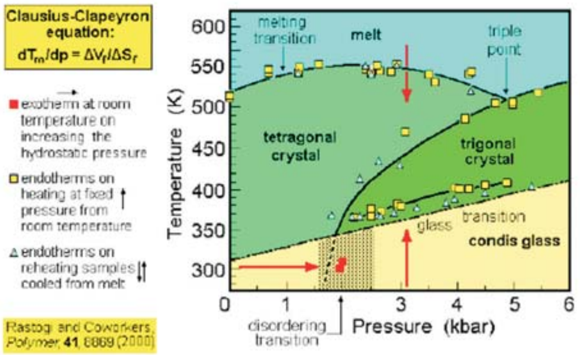

Fig. 33 Phase diagram of poly(4-methyl pentene-1)

an attempt to direct the research towards the analysis of nanophases. The work on separating single macromolecules on the liquid surface of a Langmuir trough and analysis by electron microscopy and diffraction [136] was continued and extended to electro-spray techniques followed by AFM observation [200]. Polyethylene, poly(oxyethylene), atactic and isotactic polystyrene were analyzed as glassy spheres and single crystals. It could be proven, that molten single-molecule droplets of isotactic polystyrene crystallize to a metastable, chain-folded single-crystal lamella and not to the expected equilibrium rod. Unfortunately, a technique to check the glass transition of the single-molecule glasses and the melting and annealing behavior was not available at this time, but is available now, and will be described in the next section. An initial effort was made with a commercial microcalorimeter, but we could succeed only in analyzing thin, continuous films [201]. The limits of the AFM thermocouple were evaluated, and it is still hoped that the next generation of tips for AFM will be sufficient to go to a direct thermal analysis of nanophase particles, such as the single-molecule particles [146]. In the meantime, however, it seems more likely that the chip calorimeter, to be described in 'Decoupling of chain segments of flexible macromolecules (2003–)', may be more successful in this task.

Decoupling of chain segments of flexible macromolecules (2003–)

With my retirement in 2001, the support through ORNL and UT, which covered about half of the research effort was terminated. The NSF support, however, still continued until 2003, and when submitting a final request for research funding based on the prior work under the topic of this section, support was granted to 2006. The descriptions of this work form the core of this section. The laboratory was maintained under the direction of Dr. Pyda at its old level, by both ORNL and UT, and cooperation was kept with several of the former coworkers. It was still possible to contribute about 70 papers and conference reports to the literature which will take to 2007 for final publication. Beyond this time, there is a plan to continue the teaching of the computer course on 'Thermal Analysis of Materials' [117] and to update it with news gained from the main conferences on the topic, to consult via e-mail and during occasional visits, and, may be, to solve some of the unsolved problems of decoupling. It could also be, that there is time left for some hobbies which were sadly neglected over the past 25 years.

The terms 'coupling and decoupling' along macromolecules were already mentioned in 'Reversible melting and the rigid-amorphous phase (1996–2003)'. They are to mean that the decoupled parts of long molecules must be described by different thermodynamic and mechanical parameters. The points of decoupling may collect at phase boundaries. In copolymers, they mark the change in chemical structure. In amorphous, flexible polymers they also describe points of entanglement. In macromolecular chemical processes, the term coupling is also used to describe the 'temporal behavior', as in the interaction between reversible and irreversible processes. The biological ADP to ATP conversion is a prime example. In macromolecular physical processes, a typical example of decoupling are the phase transitions and their interaction with mixing or demixing which depends on the relative rates for the sequential progress.

Naturally, there are different degrees of coupling, as became obvious when studying the RAF. In fact my attention to this concept had its beginning at the 1979 'IUPAC Symposium on Thermal Analysis' in Prague. After my lecture on the 'Thermal Properties of the Solid State', a heated discussion about the change in C_p at the glass transition of semicrystalline polymers put its additivity in doubt, and with it, the model of the two-phase model. This discussion started investigations in our laboratory [91, 92] which led to a three-phase model, with the RAF being partially decoupled at the crystal interface. The partial decoupling being caused by stress transfer which creates an amorphous nanophase with a different glass transition than the bulk phase. This description of the phase structure, as well as the concept of decoupling, is expounded in [202].

As in each of the prior sections, experimental progress is to be reported first. After summarizing the advantages, and bemoaning the frequently less-than-quantitative thermal analyses in the literature, one of the old problems in the DSC of fibers and liquids was resolved [203]. It was found that on melting, drawn fibers will shrink with such force that the sample pan deforms. This also is sometimes true when cycling a sample between solid and liquid and the sample lo-

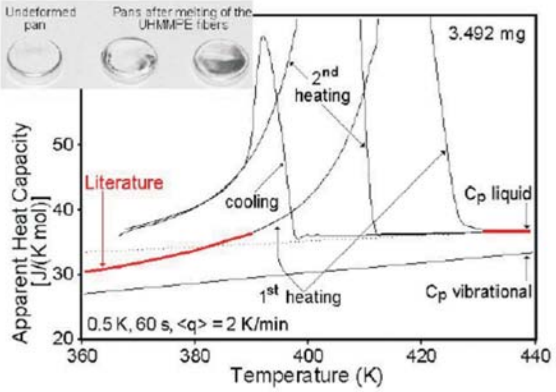

Fig. 34 Standard DSC of a gel-spun PE fiber with an initial double fit with literature data (red) before and after melting

cates itself in the crevices of the coldwelded pan. A sample must be well isolated from the pan and given enough space to change its shape, or even not be taken through the solid–liquid transition to get quality data as in Fig. 29. As an example of this problem, in Fig. 34, the precision of the literature could only be achieved by two calibrations to data of the liquid of the first heating trace. First, at low temperature, second, beyond the melting peak. Subsequent cooling and heating, then, kept the proper calibration. The deformations that the pans can suffer are shown in the top insert of Fig. 34. Only after this problem was solved, could the multi-frequency analysis of this fiber of ultra-high molar mass polyethylene be completed [204].

The main progress in instrumentation, however, did not come from the traditional makers of calorimeters, but from the manufacturers of electronic chips capable of measuring temperature on extremely small samples. The first successful calorimeters were summarized during the last two Lähnwitz Seminars in Germany in 2002 and 2004, and the 2004 NATAS Meeting in the US [205]. Our own effort on fast measurements concerned thermometry and DTA of the study of the melting kinetics of polymer crystals and the possibility of identification of the metastable polypropylene mesophase [49, 50, 103]. In these experiments, rates of temperature change of almost 10000 K min^{-1} were accomplished. From such experiments it also became clear that samples of nanogram size could be heated with rates above 10000 K s^{-1} with minimal internal temperature gradients, as were, indeed reached and exceeded with the super-fast chip calorimeters [205].

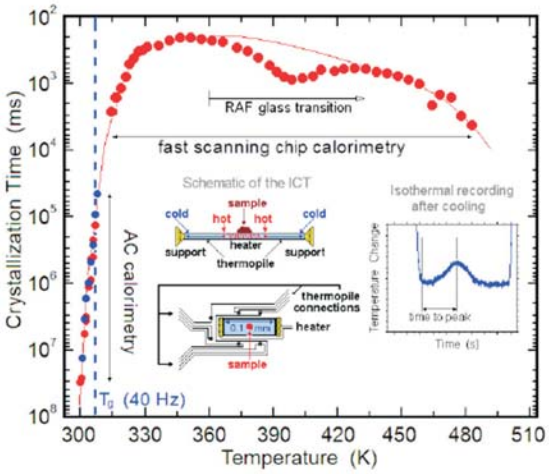

Fig. 35 Crystallization time of 0.1 μg PBT measured by ICT

Experiments with an integrated chip thermometer (ICT) were performed in the laboratory of Prof. Schick on the samples also used in the measurements shown in Fig. 30 and are displayed in Fig. 35 [175]. A side and top schematic of the ICT are drawn as inserts. The PBT was quenched with about 10^6 K s^{-1} to the crystallization temperature with a coolant gas after melting in the ICT to produce an amorphous sample. The temperature change due to crystallization was then followed at the crystallization temperature (see the insert on the right). For slow analyses of quenched samples of PBT, see also the right graph of Fig. 30. Of interest is the possible slowing of the crystallization rate by the glass transition of the RAF as marked in Fig. 30. No second crystal polymorph or change in crystal morphology is known for PBT to otherwise account for this observation.

The decoupling of crystal and surrounding amorphous material was studied with a wide range of POE samples [206]. Figure 27, above, contains the proof that the extended-chain crystals grown from low-molar-mass samples, melt fully irreversibly. The same was found for sharply folded crystals, while with a molar mass above about 10000 Da the behavior is that common for folded-chain crystals [144], and illustrated in Fig. 27 for PET. When analyzing the thermodynamic C_p of POE crystals by quasi-isothermal TMDSC, it was found that it increased to the level of the liquid before melting, indicating a ‘glass transition of the crystal’ [207]. This is presented in the upper left of Fig. 36. The glass transition temperature increased from about 310 K for the extended chain crystals of molar mass 1500 Da to 324 K for molar masses of crystals of molar mass above 20000 Da. The X-ray data in the upper right of Fig. 36 indicates no change in crystal structure up to the melt. The coherence length of the crystals, furthermore, stays constant and the unit-cell volume of the crystal increases normally up to the glass transition, and then shows an abrupt change in expansivity, as is commonly seen for glass transitions. Such behavior must drastically change the physical properties of the crystals. Normally, one would see under these conditions a disordering transition to a mesophase as shown in Fig. 13. The high mobility in POE crystals, however, is not unique, it is

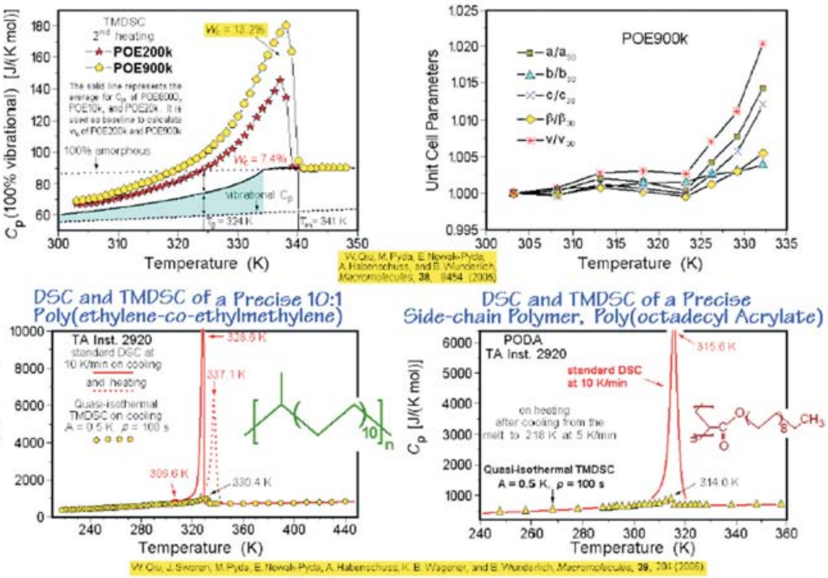

Fig. 36 Analyses by DSC, TMDSC and X-ray diffraction. Top left: apparent reversible heat capacity of POE indicating a glass transition of the crystals. Top right: X-ray data supporting a glass transition at 324 K. Bottom: apparent reversible heat capacities of two precisely constructed copolymers

also observed in nylon crystals [131, 132] where quasi-elastic neutron-scattering indicated a liquid-like mobility in parallel with an increase in C_p. These observations justify the definitions in Fig. 10. It is not the order in the crystal that makes it solid, but the cooperative freezing of the large-amplitude motion at the glass transition temperature. Only as a secondary effect does the ordering often increases the glass transition to coincide with the melting temperature, but this does not have to be the case. There can be a glass transition within a crystal before melting [207]. Locally-isolated, large-amplitude motion can also occur within crystals and cause equilibrium defects as shown for polyethylene in Figs 4 and 15.

The bottom-row of Fig. 36 illustrates the most recent advance based on the application of TMDSC to the analysis of macromolecular crystals. Precisely constructed copolymers can be produced by special synthesis. Such copolymers melt as sharply as the homopolymers which are displayed in Fig. 27. The reversible, local melting of the monoclinic crystals is much less than seen for the random copolymers and the melting temperatures are close to the temperatures of melting of paraffins which are comparable in length to the decoupled CH_2-sequences [208]. The macroconformation, however, remains that of a macromolecule, as summarized in Fig. 11, i.e., it is chain-folded at a length about three times longer than the CH_2-sequences. The decoupling at the points of the changing chemical structure is not complete, rather, the defects are collected in given planes inside the crystals. Similar precise structures with larger interruptions were analyzed earlier. In these cases, the foreign units separating the CH_2 chains were aromatic and separated as nanophases, also yielding an overall lamellar structure, again with multiple layers closely coordinated in the mesophase structure [190]. Quite in contrast to these precisely constructed polymers, are the random copolymers, studied earlier and illustrated on the left in Fig. 37 [172] with a hexyl-

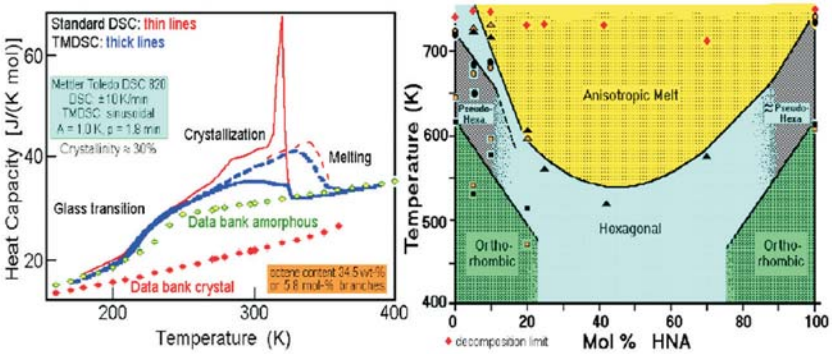

Fig. 37 Analysis of poly(ethylene-co-octene-1) with DSC and TMDSC (on the left), and the phase diagram of poly(oxybenzoate-co-naphthoate) (on the right)

branched polyethylene of similar CH_2-concentration and crystallinity. The cooling traces show a sharp peak of orthorhombic PE crystal growth, followed by a broad hexagonal crystal growth. The melting region covers about 150 K, starting within the glass transition, with a large fraction melting reversibly. Having the full spectrum from oligomers to homopolymers to random and finally precisely engineered copolymers available, it became obvious that the present knowledge about the reversible and irreversible thermodynamics of polymer crystallization is still in need of considerable further development.

As during the earlier research, the basic effort to collect quantitative information on polymeric materials was continued. First, work on the TMDSC of polytetrafluoroethylene was completed [209, 210]. It was found that the solid-solid transition of the triclinic crystals from a $2^{*}13/6$ to a $2^{*}15/7$ helix at low temperature was irreversible, while the subsequent disordering of the helix at slightly higher temperature was reversible [209]. Finally, the transition from the trigonal condis crystal to the melt is similar to the melting of polyethylene [210], i.e., the melt-crystallized, folded-chain crystals show a certain fraction of locally reversible melting, while the extended-chain crystals do not (Fig. 27).

The specific RAF of cold crystallized poly(ethylene terephthalate), i.e., the ratio between RAF and crystallinity at the subsequently measured glass transition temperature of the mobile amorphous fraction was found to decrease from almost two to 3/4 after annealing [211]. This decrease of the specific rigid amorphous fraction is due to crystal perfection, i.e., an increased decoupling of the amorphous and crystalline phases. This should be compared to the even stronger coupling of PPO in Fig. 27 (bottom left), where the specific RAF was three.

Another system involved the update and completion of the phase diagram of poly(oxybenzoate-co-naphthoate) which is illustrated at the right of Fig. 37 [212]. Due to the similar overall shape of the repeating units, a mesophase-like order is seen in the center and high-temperature areas of the diagram. Only in the vicinity of the homopolymer compositions are true crystals observed. The earlier work on the calorimetry of this and similar other copolymer systems are described in [113].

A final ATHAS effort at UT dealt with two biodegradable polymers, poly(lactic acid) and poly(vinyl methyl ether) [213]. For both the thermodynamic functions and their interpretation were added to the Data Bank, and the reversibility was probed with TMDSC. This work broadens the work on bio-related polymers, an effort to be continued by Dr. Pyda in his new location.

Conclusions

Over the last 50 years much progress has been made in the understanding and techniques of thermal analysis of polymers and my students and I were very fortunate to be part of this development. Who could have predicted in the 1950s the possibility to visualize the thermal motion by supercomputer, the ability to complete the measurement of heat capacity in less than a day, the ease with which the heat capacity of proteins can be computed from its thousands of normal mode vibration frequencies, to estimate quantities for which there are no theoretical correlations (yet) via neural net calculations, to separate reversible and irreversible processes by calorimetry, and to make measurements on nanograms of material at rates as fast as one million kelvins per second? Finally, it was difficult to imagine that 50 years later, it is possible to disseminate this advanced thermal analysis system over the internet and study the material anywhere in the world. The fields of thermal analysis and polymer science have changed and grown, but they have also become continuously more exciting than they were before. Thermal analysis is still one of the fastest growing disciplines of research and there are many instrumental and theoretical developments expected that will permit increasingly more quantitative measurements and polymer science has not yet reached the complexity of biopolymers. DTA, DSC and TMDSC has contributed much to the understanding of macromolecules [214]. In conclusion, it should be remembered that all topics mentioned in this personal review are linked in great detail to the literature in the many hundreds of references cited in the pertinent reviews [11, 45, 52, 54, 61, 62, 94, 143, 144, 215], books [21, 93, 116] and the computer course [117].

Acknowledgements

First and foremost I would like to acknowledge the more than 50 years of unwavering support through my wife, Heidi, without whom many of the projects simply could not have been completed. Similarly, our children had to grow up knowing that often research and teaching had to take precedence. Furthermore, without coworkers, little could have been accomplished. The 138 postdoctoral fellows, graduate students, and technicians contributed 330 person-years to the listed references and are to be credited for the bulk of the scientific work. Many friends and colleagues contributed with discussion, constructive criticism, and often also by joint publications. Little work can be done without this interplay of ideas. The limited space has not permitted to give a full appreciation of the importance of the ideas drawn from the literature. These hundreds of additional citations can be found in the initial papers and reviews of each of the treated subjects. Much of the knowledge about the link of fundamental polymer science to industrial applications grew out of an exclusive consultantship with several of the many research laboratories of the DuPont de Nemours Company from 1962 to 1990. Without this experience, which over time accounted for more than a year of internship, many of the connections of fundamental knowledge to applications could not have been made, and directions of research to gain ultimate understanding of existing materials would have been overlooked.

Material support was received from the three major instrument companies for thermal analysis equipment: TA Instruments, Inc.; Mettler-Toledo, Inc., and Perkin-Elmer Corp. Without this help we would not always have been able to be at the forefront of instrumentation. Major financial support for the research came from outside the universities. I estimate that over the 50 years about 5 megadollars were spent by government agencies, companies, and private foundations to support coworkers, myself during the summers until 1988, research equipment, expenses, and travel. This is a large amount of money, but not so much, if one compares it to typical expenditures in some other fields (it amounts to about 10 k$ per publication). Major sustained funding came from the Advanced Projects Agency (ARPA), the Office of Naval Research (ONR), the National Aeronautics and Space Agency (NASA), and, most prominently, the National Science Foundation (NSF, the Division of Materials Research, Polymers Program, the last Grant was # DMR-0312233), and the Division of Materials Sciences and Engineering, Office of Basic Energy Sciences, U.S. Department of Energy at Oak Ridge National Laboratory (now managed and operated by UTBattelle, LLC, for the U.S. Department of Energy, under contract number DOE-AC05-00OR22725). Industrial support was given by TA Instruments, Inc; ICI Paints; Exxon Research and Engineering Co.; Shell Development Co.; Toray Research Center and Cargill-Dow LLD.

Last, but by no means least, I would like to thank Dr. E. Turi for the invitation to write Part I of this paper and for her untiring effort to entice so many of my students and friends to contribute to the 65th birthday issue of the Journal of Thermal Analysis, and Dr. J. Menczel, who arranged the 75th birthday symposium at the 34th NATAS Meeting.

References

The second numbers listed for the references from our laboratory refer to the overall chronological list of publications that contained in June 1995 415 entries. By now (May 2006), this number has grown to 575. For additional references and new additions from the ATHAS laboratory see [83]. Multiple listings under one reference, contain all participating authors to avoid duplications when possible, but not everyone is necessarily a coauthor in each of the papers of the series.

1 146. R. Benkhoucha and B. Wunderlich, Z. Allgem. Anorg. Chemie, 444 (1978) 256; 147. R. Benkhoucha and B. Wunderlich, Z. Allg. Anorg. Chem., 444 (1978) 267.
2 M. Dole, ‘My Life in the Golden Age of America’, Vantage Press, New York, NY 1989.
3 B. Wunderlich, Thesis, Dept. Chem. Northwestern University, Evanston, IL 1957. University Microfilms, Ann Arbor, MI, Abstract 24,937, XVIII, 2, p. 424, 1958.
4 3. B. Wunderlich and M. Dole, J. Polym. Sci., 32 (1958) 125; 5. M. Dole and B. Wunderlich, Makromolekulare Chemie, 34 (1959) 29.
5 4. B. Wunderlich, J. Chem. Phys., 29 (1958) 1395.
6 W. Nernst, Der Energieinhalt fester Stoffe, Ann. Phys., 36 (1911) 395.
7 J. C. Southard and F. G. Brickwedde, J. Am. Chem. Soc., 55 (1933) 4378.
8 A. E. Worthington, P. C. Marx and M. Dole, Rev. Sci. Instrum., 26 (1955) 698.
9 F. E. Karasz, H. E. Bair and J. M. O’Reilly, J. Phys. Chem., 69 (1965) 2657.
10 F. S. Dainton, D. M. Evans, F. E. Hoare and T. P. Melia, Polymer, 3 (1962) 263, 271, 277, 286, 297, 310, 316, 317.
11 52. B. Wunderlich and H. Baur, Heat Capacities of Linear High Polymers (transl. into Russian by Yu. Godovsky, Publishing House ‘Mir’, Moscow 1972), Fortschr. Hochpolymeren Forsch, (Adv. Polym. Sci.), 7 (1970) 151.
12 M. LeBlanc and M. Kröger, Z. Elektrochem., 34 (1928) 242.
13 N. Bekkedahl and H. Matheson, J. Res. Natl. Bur. Stand., 15 (1935) 503.
14 C. T. Anderson, J. Am. Chem. Soc., 59 (1937) 1036.
15 F. T. Gucker Jr. and W. L. Ford, J. Am. Chem. Soc., 60 (1938) 2563.
16 A. Einstein, Ann. Phys., 22 (1907) 180, 800.
17 P. Debye, Ann. Phys., 37 (1912) 789.
18 V. V. Tarasov, Zh. Fiz. Khim., 24 (1950) 111.
19 W. H. Stockmayer and C. E. Hecht, J. Chem. Phys., 21 (1953) 1954.
20 The first major treatise on Polymer Science is: H. A. Stuart, ‘Die Physik der Hochpolymeren’, Vol. 14, Springer Verlag, Berlin 1952–56.
21 For a detailed review with hundreds of references to the literature up to the mid-1970s of crystals and crystallization of macromolecules see 95 and 102, B. Wunderlich, ‘Macromolecular Physics, Vols 1 and 2’, Academic Press, New York 1973 and 1976; out of print, but available as a PDF reprints from the author with a new Introduction, 2005.
22 8. B. Wunderlich and P. Sullivan, J. Polym. Sci., 56 (1962) 19.
23 9. B. Wunderlich and P. Sullivan, Polym. Sci., 61 (1962) 195; 11. B. Wunderlich and P. Sullivan, Polymer, 3 (1962) 247.
24 13. B. Wunderlich, J. Polymer Sci., Part A, 1 (1963) 1245.
25 17. B. Wunderlich and T. Arakawa, J. Polym. Sci., Part A, 2 (1964) 3697; 25. P. H. Geil, F. R. Anderson, B. Wunderlich and T. Arakawa, J. Polym. Sci., Part A, 2 (1964) 3707.
26 2. B. Wunderlich and M. Dole, J. Polym. Sci., 24 (1957) 201.
27 J. D. Hoffman, J. Am. Chem. Soc., 74 (1952) 1696.
28 K. H. Hellwege, W. Knappe and V. Semjonow, Z. Angew. Phys., 11 (1959) 285.
29 F. H. Müller and H. Martin, Kolloid-Z., 172 (1960) 97.
30 M. J. O’Neill, Anal. Chem., 36 (1964) 1238.
31 7. B. Wunderlich and W. H. Kashdan, J. Polym. Sci., 50 (1961) 71.
32 12. B. Wunderlich and D. Poland, J. Polym. Sci., Part A, 1 (1963) 357.
33 16. 28 B. Wunderlich, Polymer, 5 (1964) 125; B. Wunderlich, Polymer, 5 (1964) 611.
34 29. B. Wunderlich and D. M. Bodily, J. Polym. Sci., Part C, 6 (1964) 137.
35 23. B. Wunderlich, D. M. Bodily and M. H. Kaplan, J. Appl. Phys., 35 (1964) 95.

36 N. Hirai and H. Eyring, J. Polym. Sci., 37 (1959) 51.

37 6. B. Wunderlich, J. Phys. Chem., 64 (1960) 1052.

38 14. B. Wunderlich, J. Chem. Phys., 37 (1962) 1203; B. Wunderlich, J. Chem. Phys., 37 (1962) 1207.

39 246. H. S. Bu, W. Aycock and B. Wunderlich, Polymer, 28 (1987) 1165.

40 18. B. Wunderlich, J. Chem. Phys., 37 (1962) 2429.

41 21. B. Wunderlich, J. Polym. Sci., Part C, 1 (1963) 41.

42 Best summarized by: A. Lavoisier, 'Traité élémentaire de Chimie, présenté dans un ordre nouveau et d'après les découvertes modernes', Paris 1789. (Frequently reprinted, see for example the English translation of Kerr, Dover Publications, New York 1965.)

43 J. Dalton, 'A New System of Chemical Philosophy', Manchester, England 1808. (Frequently reprinted, see for example The Citadel Press, New York 1964, The Science Classics Library.)

44 See for example 'The Scientific Papers of J. Willard Gibbs', Dover Publications, New York, NY 1961 and later.

45 350. B. G. Sumpter, D. W. Noid, G. L. Liang and B. Wunderlich, 'Atomistic Dynamics of Macromolecular Crystals', Published in the special volume on 'Atomistic Modelling of Physical Properties of Polymers, U. Suter and L. Monnerie, Eds, Adv. Polym. Sci., 116 (1994) 27–72; see also: 504. B. Wunderlich, M. Pyda, J. Pak and R. Androsch, Thermochim. Acta, 377 (2001) 9.

46 38. B. Wunderlich, J. Phys. Chem., 69 (1965) 2078.

47 36. T. Arakawa and B. Wunderlich, J. Polym. Sci., Part C, 16 (1967) 653; 45, 49. C. M. Cormier and B. Wunderlich, J. Polym. Sci., Part A-2, (1966) 666; C. M. Cormier and B. Wunderlich, J. Polym. Sci., Part A-2, (1967) 987.

48 317. Y. Jin and B. Wunderlich, J. Phys. Chem., 95 (1991) 9000.

49 34. E. Hellmuth and B. Wunderlich, J. Appl. Phys., 36 (1965) 3039.

50 43. B. Wunderlich and E. Hellmuth, Superheating Studies on Polymer Crystals. Proc. 1st ICTA, Thermal Analysis, J. P. Redfern, Ed., MacMillan and Co., Ltd., p. 76, London 1965; 66. M. Jaffe and B. Wunderlich, Superheating of Extended-Chain Polymer Crystals. Proc. 2nd ICTA, Thermal Analysis, Vol. 1, p. 387, E. F. Schwenker and P. D. Garn, Eds, Academic Press, New York 1969.

51 68, 48, 69, 47, 70, 67, 84, 89, 90. B. Wunderlich *et al*., Extended-Chain Crystals, J. Polym. Sci., Part A-2, 7 (1969); with T. Davidson, I. General Crystallization Conditions and Review of Pressure Crystallization of Polyethylene, p. 2043; II. Crystallization of Polyethylene under Elevated Pressure, p. 2051; with R. B. Prime III. Size Distribution of Polyethylene Crystals Grown under Elevated Pressure, p. 2061; IV. Melting under Equilibrium Conditions, p. 2073; with R. B. Prime and L. Melillo, V. Thermal Analysis and Electron Microscopy of the Melting Process in Polyethylene, p. 2091; with C. L. Gruner and R. C. Bopp, VI. Annealing of Polyethylene under Elevated Pressure, p. 2099; with M. C. Coughlin, VII. Lamellar and Fibrillar Spherulites in Selenium. J. Polym. Sci., Polymer Letters Ed., 10 (1972) 57; withL. Melillo, VIII. Kolloid Z. Z. Polymere, 250 (1972) 417; with M. C. Coughlin, IX. Kolloid Z. Z. Polymere, 250 (1972) 482.

52 61. B. Wunderlich, Fortschr. Hochpolymeren Forsch., (Adv. Polym. Sci.), 5 (1968) 568.

53 113. B. Wunderlich and A. Mehta, J. Polym. Sci., Polym. Phys. Ed., 12 (1974) 255.

54 53. B. Wunderlich, Differential Thermal Analysis, Physical Methods of Chemistry, A. Weissberger and B. W. Rossiter, Eds Vol. 1, Part V, Chapter 8, p. 427, John Wiley & Sons, Inc., New York 1971.

55 108, 109, 124, 184. B. Wunderlich, Texts and Audio Courses. Crystals of Linear Macromolecules, p. 235, Am. Chem. Soc., Washington, DC 1973. The later audio courses were published by Rensselaer Polytechnic Institute, Troy, NY: Thermal Analysis of Linear Macromolecules, p. 175, 1973 (second printing 1975); Crystallization of Linear Macromolecules, p. 225, 1975; Thermal Analysis, p. 288+xiv, 1981.

56 44. B. Wunderlich and C. M. Cormier, J. Phys. Chem., 70 (1966) 1844.

57 50. B. Wunderlich, L. Melillo, C. M. Cormier, T. Davidson and G. Snyder, J. Macromol. Sci., B1 (1967) 485.

58 63. B. Wunderlich and L. Melillo, Makromol. Chem., 118 (1968) 250.

59 F. L. Binsbergen, Kolloid Z. Z. Polymere, 238 (1970) 389.

60 D. C. Bassett and B. Turner, Nature (London) Phys. Sci., 240 (1970) 146.

61 200. B. Wunderlich and J. Grebowicz, Adv. Polym. Sci., 60/61 (1984) 1.

62 263. B. Wunderlich, M. Möller, J. Grebowicz and H. Baur, 'Conformational Motion and Disorder in Low and High Molecular Mass Crystals', Springer Verlag, Berlin 1988, (Adv. Polymer Sci., Vol. 87).

63 56. M. Jaffe and B. Wunderlich, Kolloid Z. Z. Polymere, 216–217 (1967) 203.

64 85. S. Kubo and B. Wunderlich, J. Polym. Sci., Polym. Phys. Ed., 10 (1972) 1949.

65 117. M. Mucha and B. Wunderlich, J. Polym. Sci., Polymer Phys. Ed., 12 (1974) 1993.

66 112. A. Mehta and B. Wunderlich, Colloid Polym. Sci., 253 (1975) 193.

67 160. B. Wunderlich, Disc. Farad. Soc., 68 (1979) 239.

68 228, 230, 267. S. Z. D. Cheng and B. Wunderlich, J. Polym. Sci., Part B, Polym. Phys., 24 (1986) 577; S. Z. D. Cheng and B. Wunderlich, J. Polym. Sci., Part B, Polym. Phys. 24 (1986) 595; S. Z. D. Cheng, H. S. Bu and B. Wunderlich, J. Polym. Sci., Part B, Polym. Phys., 26 (1988) 1947.

69 75, 88, 96. A. Miyagi and B. Wunderlich, J. Polym. Sci., Polym. Phys. Ed., 10 (1972) 2073; A. Miyagi and B. Wunderlich, J. Polym. Sci., Polym. Phys. Ed., 10 (1972) 1401; A. Miyagi and B. Wunderlich, J. Polym. Sci., Polym. Phys. Ed., 10 (1972) 2085.

70 104. M. C. Coughlin and B. Wunderlich, J. Polym. Sci., Polym. Phys. Ed., 11 (1973) 1735.

71 114. R. Iwamoto, R. C. Bopp and B. Wunderlich, J. Polym. Sci., Polym. Phys. Ed., 13 (1975) 1925.

72 60. F. N. Liberti and B. Wunderlich, J. Polym. Sci., Part A-2, 6 (1968) 833.

73 42. E. Hellmuth, B. Wunderlich and J. M. Rankin, Appl. Polym. Symposia, 2 (1966) 101.

74 72. T. G. Coker, B. Wunderlich and G. J. Janz, Trans. Farad. Soc., 65 (1969) 3361.

75 78. S. M. Wolpert, A. Weitz and B. Wunderlich, J. Polym. Sci., Part A-2, 9 (1971) 1887.

76 116. A. Weitz and B. Wunderlich, J. Polym. Sci., Polym. Phys. Ed., 12 (1974) 2473.

77 110. A. Mehta and B. Wunderlich, Makromol. Chem., 175 (1974) 977.

78 130. A. Mehta and B. Wunderlich, Am. Chem. Soc., 35 (1975) 393; 138. U. Gaur, A. Mehta and B. Wunderlich, J. Thermal Anal., 13 (1978) 71.

79 195. B. Wunderlich, Am. Lab., 14 (1982) 28.

80 257. B. Wunderlich and P. Fellner, Thermochim. Acta, 110 (1987) 67.

81 204. B. Wunderlich, Computer Course and Text: Introduction to Differential Thermal Analysis, Rensselaer Polytechnic Institute, Troy, NY 1983. For the more recent effort in computer courses on thermal analysis see [117].

82 151, 153, 159, 171, 177, 180, 289. U. Gaur, H.-C. Shu, A. Mehta, S.-F. Lau, B. B. Wunderlich, M. Varma-Nair and B. Wunderlich, J. Phys. Chem., Ref. Data, 10 (1981) 89 119 1001 1051; 11 (1982) 313 1065; 12 (1983) 29, 65, 91; 20 (1991) 349.

83 The ATHAS website is: http://web.utk.edu/~athas, A general description is given in: 370. B. Wunderlich, Pure Appl. Chem., 67 (1995) 1019 and 276. B. Wunderlich and M. Pyda, J. I. Kroschwitz, Ed. 'Encyclopedia of Polymer Science and Engineering', 3rd Ed., p. 43, John Wiley & Sons, DOI: 10.1002/0471440264. PST 369 (2004). Also available via: www.mrw.interscience.wiley.com/epst. For the ATHAS data bank see also: http://www.evitherm.org/index.asp.

84 216. J. Grebowicz and B. Wunderlich, J. Thermal Anal., 30 (1985) 229; 285. R. Pan, M. Varma and B. Wunderlich, J. Thermal Anal., 35 (1989) 955.

85 191. Yu. V. Cheban, S.-F. Lau and B. Wunderlich, Colloid Polym. Sci., 260 (1982) 9; 207. S.-F. Lau and B. Wunderlich, J. Thermal Anal., 28 (1983) 59; 269. R. Pan, M. Varma-Nair and B. Wunderlich, J. Thermal Anal., 36 (1990) 145; 258. H. S. Bu, S. Z. D. Cheng and B. Wunderlich, J. Phys. Chem., 91 (1987) 4179. Recent advances are: 412. G. Zhang and B. Wunderlich, J. Thermal Anal., 47 (1996) 899; 443. M. Pyda, M. Bartkowiak and B. Wunderlich, J. Therm. Anal. Cal., 52 (1998) 631.

86 260. K. Loufakis and B. Wunderlich, J. Phys. Chem., 92 (1988) 4205. For further developments see [193].

87 231, 249. U. Gaur, M.-Y. Cao, R. Pan and B. Wunderlich, J. Thermal Anal., 31 (1986) 421; J. Thermal Anal., 31 (1986) 1319.

88 169. U. Gaur and B. Wunderlich, Macromolecules, 13 (1980) 1618; 196. S.-F. Lau, J. Pathak and B. Wunderlich, Macromolecules, 15 (1982) 1278.

89 90. R. C. Bopp, U. Gaur, R. P. Kambour and B. Wunderlich, J. Thermal Anal., 25 (1982) 243.

90 205. S.-F. Lau, J. Wesson and B. Wunderlich, Macromolecules, 17 (1984) 1102.

91 170. J. Menczel and B. Wunderlich, J. Polym. Sci., Polym. Lett. Ed., 19 (1981) 261.

92 219. H. Suzuki, J. Grebowicz and B. Wunderlich, Br. Polym. J., 17 (1985) 1.

93 123. B. Wunderlich, Macromolecular Physics, Vol. 3, Crystal Melting, Academic Press, p. 363, New York, London, (translated into Russian, MIR, Moscow 1984), 1980, now available as a PDF reprint, 2005.

94 141. B. Wunderlich, Thermal Characterization of Polymeric Materials, E. Turi, Ed., Academic Press, New York 1981, pp. 91–234; revised 2nd Ed., 1997, pp. 205–482.

95 255. B. Wunderlich, Workbook: Chemistry 2000, Rensselaer Polytechnic Institute, Troy, NY 1987, p. 306+xii.

96 150. B. Wunderlich and H.-C. Shu, J. Crystal Growth, 48 (1980) 227; 154. H.-C. Shu, U. Gaur and B. Wunderlich, J. Polym. Sci., Polym. Phys. Ed., 18 (1980) 449.

97 176. U. Gaur, G. Pultz, H. Wiedemeier and B. Wunderlich, J. Thermal Anal., 21 (1981) 309.

98 136. B. Wunderlich and G. Czornyj, Macromolecules, 10 (1977) 906; 166. U. Gaur and B. Wunderlich, Macromolecules, 13 (1980) 445.

99 139. A. Mehta, U. Gaur and B. Wunderlich, J. Polym. Sci., Polym. Phys. Ed., 16 (1978) 289.

100 144. P. C. Jain, B. Wunderlich and D. R. Chaubey, J. Polym. Sci., Polym. Phys. Ed., 15 (1977) 2271.

101 264. S. Z. D. Cheng and B. Wunderlich, Macromolecules, 22 (1989) 1866.

102 206. S.-F. Lau, H. Suzuki and B. Wunderlich, J. Polym. Sci., Polym. Phys. Ed., 22 (1984) 379; 360. Y. Jin, A. Boller, B. Wunderlich and B. V. Lebedev, Thermochim. Acta, 234 (1994) 103; 262. K. Loufakis and B. Wunderlich, Macromolecules, 20 (1987) 2474.

103 189. J. Grebowicz, S.-F. Lau and B. Wunderlich, J. Polym. Sci., Symposia, 71 (1984) 19; 277. H. S. Bu, S. Z. D. Cheng and B. Wunderlich, Rapid Commun., 9 (1988) 75; 259. Z. Q. Wu, V. L. Dann, S. Z. D. Cheng and B. Wunderlich, J. Thermal Anal., 34 (1988) 105.

104 223, 224. D. E. Kirkpatrick and B. Wunderlich, Makromol. Chem., 186 (1985) 2595; J. Polym. Sci., Part B, Polym. Phys., 24 (1986) 931.

105 251. S. Z. D. Cheng, M.-Y. Cao and B. Wunderlich, Macromolecules, 19 (1986) 1868.

106 254. S. Z. D. Cheng and B. Wunderlich, Macromolecules, 20 (1987) 1630.

107 270. S. Z. D. Cheng and B. Wunderlich, Macromolecules, 21 (1988) 789.

108 278. S. Z. D. Cheng, R. Pan and B. Wunderlich, Makromol. Chem., 189 (1988) 2443.

109 256. S. Z. D. Cheng, Z. Q. Wu and B. Wunderlich, Macromolecules, 20 (1987) 2801; 245. S. Z. D. Cheng, S. Lim, L. H. Judovits and B. Wunderlich, Polymer, 28 (1987) 10.

110 C. Robinson, Trans. Farad. Soc., 52 (1956) 571.

111 P. J. Flory, Proc. Roy. Soc., A234, 60 (1956) 73.

112 A. Roviello and A. Siguru, J. Polym. Sci., Polym. Lett. Ed., 13 (1975) 455.

113 165, 173, 192, 188, 215, 194, 293. J. Menczel, W. Meesiri, U. Gaur, J. Grebowicz, M.-Y. Cao, M. Varma-Nair and B. Wunderlich, J. Polym. Sci., Polym. Phys. Ed., 18 (1980) 1433; Polymer, 22 (1981)

778; J. Menczel, W. Meesiri, U. Gaur, J. Grebowicz, M.-Y. Cao, M. Varma-Nair and B. Wunderlich, J. Polym. Sci., Polym. Phys. Ed., 20 (1982) 719; J. Mol. Cryst. Liq. Cryst., 76 (1981) 287; J. Polym. Sci., Part B, Polym. Phys., 23 (1985) 521. J. Polym. Sci., Part B, Polym. Phys., 21 (1983) 141; J. Polym. Sci., Part B, Polym. Phys., 1 (1990) 151.

114 236–239, 333, 368: (Condis Crystals of Small Molecules, Parts I–VI). B. Wunderlich, M. Möller, H. G. Wiedemann, J. Grebowicz, M. Y. Cao, J. Wesson, K. Loufakis, M. Möller, D. Oelfin, J. Cheng, Y. Jin, G. Liang and W. Chen, Mol. Cryst. Liq. Cryst., 140 (1986) 211; Mol. Cryst. Liq. Cryst., 140 (1986) 219; Mol. Cryst. Liq. Cryst., 140 (1986) 231; Mol. Cryst. Liq. Cryst., 173 (1989) 101; Mol. Cryst. Liq. Cryst., 213 (1992) 237; Mol. Cryst. Liq. Cryst., 241 (1994) 299.

115 290. B. Wunderlich, 'Thermal Analysis', Academic Press, New York, NY 1990, pp. 450+xvi, An expansion and update of this book is [116].

116 500. 'Thermal Analysis of Polymeric Materials', 947 figures. Springer Verlag, Berlin 2005, pp. 894+xvi.

117 393, 560. B. Wunderlich, 'Physical Chemistry of Polymers', Figures, text and hypertext of a computer-assisted course of thousands of screens. After many updates and expansions, this computer course is now available as 560, 'Thermal Analysis of Materials', A computer-assisted lecture course of 36 lectures, Updated and changed to newly developed presentation software, published via the Internet (2005–2006). Available by downloading from the site: http://web.utk.edu/~athas, or also from the European Virtual Institute for Thermal Metrology at its site: http://www.evitherm.org/index.asp, their home page for thermal analysis and calorimetry.

118 253. B. Wunderlich, J. Thermal Anal., 32 (1987) 1949; 298, 307, 331. Y. Jin and B. Wunderlich, J. Thermal. Anal., 36 (1990) 765; Y. Jin and B. Wunderlich, J. Thermal Anal.,36 (1990) 1519; Y. Jin and B. Wunderlich, J. Thermal Anal., 38 (1992) 2257.

119 S. R. Sauerbrunn, B. S. Crowe and M. Reading, 21st Proc. NATAS Conf. in Atlanta GA, Sept. 1316 (1992); M. Reading, B. K. Hahn and B. S. Crowe, US Patent 5,224,775, July 6, 1993, p. 137.

120 385, 378, 391. B. Wunderlich, Y. Jin, C. Schick and A. Boller, Thermochim. Acta, 238 (1994) 277; J. Thermal Anal., 42 (1994) 307; Modulated Differential Thermal Analysis in the Glass Transition Range, Proc. 23rd NATAS Conf., in Toronto, Canada, Sept. 25–28, 1994; Thermochim. Acta, 266 (1995) 97.

121 W. Pechhold, Kolloid Z. Z. Polymere, 228 (1968) 1.

122 320, 349, 384, 397, 398. B. Wunderlich, A. Xenopoulos, D. W. Noid, B. G. Sumpter, G. L. Liang and S. N. Kreitmeier, Defect Generation and Motion in Polyethylene-like Crystals, Analyzed by Simulation with Supercomputers, P. D. Bristowe, J. E. Epperson, J. E. Griffith and Z. Lilienthal-Weber, Eds, Defects in Materials. Proc. of the 1990 Fall Meeting of the Mat. Res. Soc., Vol. 209, p. 147 (1991); Macromolecules, 25 (1992) 7247; J. Phys. Chem., 98 (1994) 11739; Faraday Trans., 91 (1995) 2601; Polym. Int., 36 (1995) 155.

123 308, 341, 325, 344, 345, 382. A. Xenopoulos, J. Cheng, M. Yasuniwa and B. Wunderlich, Mol. Cryst. Liq. Cryst., 214 (1992) 63; J. Cheng, A. Xenopoulos and B. Wunderlich, Mol. Cryst. Liq. Cryst., 220 (1992) 105; J. Cheng, A. Xenopoulos and B. Wunderlich, Mol. Cryst. Liq. Cryst., 220 (1992) 127; J. Cheng, A. Xenopoulos and B. Wunderlich, 225 (1992) 337; A. Xenopoulos, J. Cheng and B. Wunderlich, Mol. Cryst. Liq. Cryst., 226 (1993) 87; Q. Wang, A. Xenopoulos and B. Wunderlich, Mol. Cryst. Liq. Cryst., 264 (1995) 115.

124 399. B. Wunderlich and W. Chen, The Difference Between Liquid Crystals and Conformationally Disordered Crystals, Presented at the Spring 1995 ACS Meeting in Anaheim, CA, A. I. Isayev, T. Kyu and S. Z. D. Cheng, Eds, 'Recent Advances in Liquid Crystalline Polymers', ACS Symposium Series, Washington, DC 1996, pp. 632, 232–248.

125 334, 335, 343. J. Cheng, Y. Jin, B. Wunderlich, S. Z. D. Cheng, M. A. Yandrasits, A. Zhang and V. Percec, Macromolecules, 25 (1992) 5991; J. Cheng, Y. Jin, B. Wunderlich, S. Z. D. Cheng, A. Zhang and V. Percec, Macromolecules, 25 (1992) 2112; Y. Jin, J. Cheng, B. Wunderlich, S. Z. D. Cheng and M. A. Yandrasits, Polymers for Advanced Technology, 5 (1994) 785;
362. J. Cheng, Y. Jin, W. Chen, B. Wunderlich, H. Jonsson, A. Hult and U. W. Gedde, J. Polym. Sci., Part B: Polym. Phys., 32 (1994) 721.

126 125. G. Czornyj and B. Wunderlich, Makromol. Chem., 178 (1977) 843.

127 283. J. Grebowicz, R. Pan and B. Wunderlich, J. Appl. Polym. Sci., 38 (1989) 707.

128 364–366. Y. Fu, W. R. Busing, Y. Jin, K. A. Affholter, A. Boller and B. Wunderlich, Macromolecules, 26 (1993) 2187; Makromol. Chem., 195 (1994) 803; J. Polym. Sci., Part B: Polym. Phys., 32 (1994) 2289.

129 390, 404, 527. W. Chen, Y. Fu, J. Cheng, A. Boller, M. Pyda, D. Londono, B. Annis, J. Pak and B. Wunderlich, J. Polym. Sci., Phys. Ed., 32 (1994) 2661; J. Macromol. Sci., Part B, B35 (1996) 37; Thermochim. Acta, 421 (2004) 203.

130 281, 299. A. Xenopoulos and B. Wunderlich, Polymer, 31 (1990) 1260; J. Polym. Sci., Part B, Polym. Phys., 28 (1990) 2271. Recent TMDSC experiments proving these interpretations are given in: 573. W. Qiu, A. Habenschuss and B. Wunderlich, The Phase and Crystal Structure of Nylon 6.6. Polymer, submitted Dec. (2006).

131 314. A. Xenopoulos and B. Wunderlich, Colloid Polym. Sci., 269 (1991) 375.

132 315. A. Xenopoulos, B. Wunderlich and A. H. Narten, Macromolecules, 26 (1993) 1576.

133 313, 339, 340. K. Roles and B. Wunderlich, Biopolymers, 31 (1991) 477; K. Roles, A. Xenopoulos and B. Wunderlich, Biopolymers, 33 (1993) 753; K. A. Roles and B. Wunderlich, J. Polym. Sci., Part B. Polym. Phys., 31 (1993) 279.

134 386, 387. G. Zhang, S. Gerdes, B. V. Lebedev and B. Wunderlich, Molecular Chem. Phys., 197 (1996) 3791; J. Polym. Sci., Part B: Polym. Phys., 33 (1995) 2445.

135 133. G. Czornyj and B. Wunderlich, J. Polym. Sci., Polym. Phys. Ed., 15 (1977) 1905.

136 300. H. Bu, Y. Pang, D. Song, Y. Yu, T. Voll, G. Czornyj and B. Wunderlich, J. Polym. Sci., Part B, Polym. Phys., 29 (1991) 139; 374. H. Bu, E. Chen, S. Xu, K. Guo and B. Wunderlich, J. Polym. Sci., Part B, Polym. Phys., 32 (1994) 1351.

137 336. B. K. Annis and B. Wunderlich, J. Polym. Sci., Part B. Polym. Phys., 31 (1993) 93; 337. B. K. Annis, D. W. Schwark, J. R. Reffner, E. L. Thomas and B. Wunderlich, Makromol. Chem., 193 (1992) 2589; 388. Q. Wang, B. Annis and B. Wunderlich, J. Polym. Sci., Part B: Polym. Phys., 32 (1994) 2653.

138 346. Y. Jin, J. Cheng, M. Varma-Nair, G. Liang, Y. Fu, B. Wunderlich, X.-D. Xiang, R. Motovoy and A. K. Zettl, J. Phys. Chem., 96 (1992) 5151.

139 371, 372. Y. Jin, A. Xenopoulos, J. Cheng, W. Chen, B. Wunderlich, M. Diack, C. Jin, R. L. Hettich, R. N. Compton and G. Guiochon, Mol. Cryst. Liq. Cryst., 257 (1994) 235; Y. Jin, A. Xenopoulos, J. Cheng, W. Chen, B. Wunderlich, M. Diack, C. Jin, R. L. Hettich, R. N. Compton and G. Guiochon, Mol. Cryst. Liq. Cryst., 257 (1994) 350.

140 319. J. A. Darsey, D. W. Noid, B. Wunderlich and L. Tsoukalas, Makromol. Chem. Rapid Commun., 12 (1991) 325; 328. D. W. Noid, M. Varma-Nair, B. Wunderlich and J. A. Darsey, J. Thermal Anal., 37 (1991) 2295.

141 407. B. Wunderlich, Thermochim. Acta, 340/41 (1999) 37.

142 433. B. Wunderlich. Macromol. Symp., 113 (1997) 51.

143 440. W. Chen and B. Wunderlich, Macromol. Chem. Phys., 200 (1999) 283.

144 522. B. Wunderlich, Progr. Polym. Sci., 28/3 (2003) 383.

145 478, 547. B. Wunderlich, J. Therm. Anal. Cal., 59 (2000) 7; Int. J. Thermophys. and Fluid Phase Eq., accepted for publication in (2007).

146 450. B. Wunderlich, Thermochim. Acta, 355 (2000) 43.

147 422, 438. A. Boller, I. Okazaki, K. Ishikiriyama, G. Zhang and B. Wunderlich, J. Thermal Anal., 49 (1997) 1081; K. Ishikiriyama and B. Wunderlich, J. Thermal Anal., 50 (1997) 337.

148 L. Waguespack and R. L. Blaine, Design of A New DSC Cell with Tzero™ Technology. Proc. 29th NATAS Conf. in St. Louis, MO, Sept 24–26, K. J. Kociba and B. J. Kociba, Eds, 29 (2001) 721; R. L. Danley, Thermochim. Acta, 395 (2003) 201.

149 468. I. Moon, R. Androsch and B. Wunderlich, Thermochim. Acta, 357/358 (2000) 285.

150 479, 482. R. Androsch, I. Moon, S. Kreitmeier and B. Wunderlich, Thermochim. Acta, 357/358 (2000) 267; Thermochim. Acta, 333 (1999) 27.

151 510, 516. W. Hu, A. Buzin, J.-S. Lin and B. Wunderlich, J. Therm. Anal. Cal., 66 (2001) 677; J. Polym. Sci., Part B: Polym. Phys., 41 (2003) 403.

152 475, 503. B. Wunderlich, R. Androsch, M. Pyda and Y. K. Kwon, Thermochim. Acta, 348 (2000) 181; P. Kamasa, M. Merzlyakov, M. Pyda, J. Pak, C. Schick and B. Wunderlich, Thermochim. Acta., 392/393 (2002) 195. For multifrequency TMDSC see also: M. Schubnell, Ch. Heitz, TH. Hütter and J. E. K. Schawe, 'TOPEM–The New Multifrequency TMDSC Technique', Proc. 33rd NATAS Conference, M. J. Rich, Ed., CD edition (2005).

153 491, 492, 495. J. Pak, Y. K. Kwon, R. Androsch, M. Pyda and B. Wunderlich, Thermochim. Acta, 367/368 (2001) 229; Thermochim. Acta, 367/368 (2001) 217; Thermochim. Acta, 367/368 (2001) 203.

154 392. M. Varma-Nair and B. Wunderlich, J. Thermal Anal., 46 (1996) 879.

155 484, 488. R. Androsch, M. Pyda, H. Wang and B. Wunderlich, J. Therm. Anal. Cal., 61 (2000) 661; Application of IR Imaging During Temperature-modulated Differential Scanning Calorimetry (TMDSC) Measurements, Proc. SPIE-Int. Soc. Opt. Eng., 4710 (2002) 44.

156 514, 515. P. Kamasa, A. Buzin, M. Pyda and B. Wunderlich, Thermochim. Acta, 381 (2002) 139; Thermochim. Acta, 396 (2003) 109.

157 420, 480, 523. M. L. Di Lorenzo and B. Wunderlich, J. Thermal Anal., 48 (1997) 207; J. Therm. Anal. Cal., 57 (1999) 459; Thermochim. Acta, 405 (2003) 255.

158 415, 427, 451. B. Wunderlich, A. Boller, I. Okazaki, K. Ishikiriyama, S. Kreitmeier and H. Baur, Thermochim. Acta 282/283 (1996) 143; Thermochim. Acta, 304/305 (1997) 125; J. Therm. Anal. Cal., 54 (1998) 437.

159 M. Merzlyakov and C. Schick, Thermochim. Acta, 330 (1999) 55.

160 447. A. Boller, M. Ribeiro and B. Wunderlich, J. Therm. Anal. Cal., 54 (1998) 545.

161 416, 414, 417, 424, 426. B. Wunderlich, A. Boller, I. Okazaki L. C. Thomas and S. Kreitmeier, J. Thermal Anal., 47 (1996) 1013; Thermochim. Acta, 284 (1996) 1; Thermochim. Acta, 291 (1997) 85; J. Polym. Sci., Part B: Polym. Phys., 34 (1996) 2941; J. Thermal Anal., 49 (1997) 57.

162 H. Eyring, J. Chem. Phys., 4 (1936) 283; J. Frenkel, 'Kinetic Theory of Liquids', Clarendon, Oxford 1946.

163 439, 498, 501. R. K. Ishikiriyama, A. Boller, Androsch and B. Wunderlich, J. Thermal Anal., 50 (1997) 547; Thermochim. Acta, 364 (2000) 181; Thermochim. Acta, 369 (2001) 67.

164 467, 458. J. Pak, A. Boller, I. Moon, M. Pyda and B. Wunderlich, Thermochim. Acta, 357/358 (2000) 259; J. Polym. Sci., Part B: Polym. Phys., 38 (2000) 2810.

165 455, 469. W. Chen, M. Dadmun, G. Zhang, A. Boller, A. Toda, I.-K. Moon and B. Wunderlich, Thermochim. Acta., 324 (1998) 87; J. Polym. Sci., Part B: Polym. Phys., 37 (1999) 1539.

166 506, 517. J. Pak, M. Pyda and B. Wunderlich, Macromolecules, 34 (2001) 4492; Thermochim. Acta, 396 (2003) 43.

167 444, 445. K. Ishikiriyama and B. Wunderlich, J. Polym. Sci., Part B, Polym. Phys., 35 (1997) 1877; Macromolecules, 30 (1997) 4126.

168 525. J. Pak and B. Wunderlich, J. Polym. Sci., Part B: Polym. Phys., 40 (2002) 2219.

169 J. Pak, M. Pyda and B. Wunderlich, Macromolecules, 36 (2003) 495.

170 437, 441, 459, 476. I. Okazaki, C. Schick, M. Merzlyakov, A. Boller, K. Ishikiriyama, W. Chen, M. Pyda, J. Pak, I. Moon, R. Androsch and B. Wunderlich, Macromolecules, 30 (1997) 1758;

Macromol. Chem. Phys., Rapid Commun., 18 (1997) 313; Polym. Bull., 40 (1998) 297; Thermochim. Acta, 330 (1999) 21.
171 527, 533, J. Pack, R. Androsch, M. Pyda and B. Wunderlich, Thermochim. Acta, 421 (2004) 203; J. Polym. Sci., Part B: Polym. Phys., 41 (2003) 2157.
172 481, 486, 496, 521. R. Androsch, J. Blackwell, S. N. Chvalun, T. Lüpke, A. Wutzler and B. Wunderlich, Macromolecules, 32 (1999) 3735; Macromolecules, 32 (1999) 7238; Macromolecules, 33 (2000) 9076; J. Polym. Sci., Part B: Polym. Phys., 40 (2002) 1223.
173 502. M. Pyda, M. L. Di Lorenzo, J. Pak, P. Kamasa, A. Buzin, J. Grebowicz and B. Wunderlich, J. Polym. Sci.: Part B: Polym. Phys., 39 (2001) 1565.
174 490. M. Pyda and B. Wunderlich, J. Polym. Sci., Part B: Polym. Phys., 38 (2000) 622.
175 548. M. Pyda, E. Nowak-Pyda, J. Heeg, H. Huth, A. A. Minakov, M. L. Di Lorenzo, C. Schick and B. Wunderlich, J. Polym. Sci., Part B: Polym. Phys., in print (2006).
176 511, 519. R. Androsch and B. Wunderlich, Macromolecules, 34 (2001) 5950; R. Androsch and B. Wunderlich, Macromolecules, 34 (2001) 8384.
177 512, 526. R. Androsch and B. Wunderlich, Thermochim. Acta, 396 (2003) 33; J. Polym. Sci., Part B: Polym. Phys., 41 (2003) 2039.
178 Y. Nukuchina, Y. Itoh and E. W. Fischer, J. Polym. Sci., B3 (1965) 383; E. W. Fischer, Pure Appl. Chem., 31 (1972) 113; J. M. Schultz, E. W. Fischer, O. Schaumburg and H. A. Zachmann, J. Polym. Sci., Polym. Phys. Ed., 18 (1980) 2390.
179 A. Toda, C. Tomita, M. Hikosaka, T. Arita and Y. Saruyama, Polymer, 39 (1998) 5093; Polym. J., 31 (1999) 790; Thermochim. Acta, 324 (1998) 95; Thermochim. Acta, 330 (1999) 75.
180 494. W. Chen, I.-K. Moon and B. Wunderlich, Polymer, 41 (2000) 4119.
181 P. Ehrenfest, Phase Changes in the Ordinary and Extended Sense Classified According to the Corresponding Singularities of the Thermodynamic Potential. Proc. Acad. Sci., Amsterdam 1933, 36, 153, Suppl 75b, Mitt. Kammerlingh Onnes Inst., Leiden.
182 P. W. Bridgman, 'The Logic of Modern Physics'; MacMillan, New York 1927; reprinted by Arno Press, New York 1980.
183 485. B. Wunderlich and I. Moon, Analysis of the Nanophase Structure of Semicrystalline Polymers with Atomic Force Microscopy, Microcalorimetry, and Temperature-Modulated Calorimetry, Proc. 27th NATAS Conf. in Savannah, GA, K. R. Williams and K. Kociba, Eds, 27 (1999) 105.
184 M. Kunz, M. Möller, U.-R. Heinrich and H.-J. Cantow, Makromol. Chem. Symposia, 20/21 (1988) 147; M. Kunz, M. Möller, U.-R. Heinrich and H.-J. Cantow, Makromol. Chem. Symposia, 23 (1989) 57; R. Kitamaru, F. Horii and K. Murayama, Macromolecules, 19 (1986) 636.
185 448. Y. K. Kwon, A. Boller, M. Pyda and B. Wunderlich, Polymer, 41 (2000) 6237.
186 C. Schick, A. Wurm and A. Mohammed, Colloid Polym. Sci., 279 (2001) 800.
187 428, 429. B. V. Lebedev, V. G. Vasil'ev, T. A. Bykova, E. G. Kiparisova, N. N. Smirnova and B. Wunderlich, Vysokomol. Soedin., A38 (1996) 216, English translation: Polym. Sci. Ser. A, 38 (1996) 104; Vysokomol. Soedin., A38 (1996) 210, English translation: Polym. Sci. Ser. A., 99 (1996).
188 435, 452, 540. K. Ishikiriyama, M. Pyda, G. Zhang, T. Forschner, A. Boller, H. Chuah, B. V. Lebedev, E. Nowak-Pyda, J. Mays, J. Grebowicz and B. Wunderlich, J. Macromol. Sci.-Phys., B37 (1998) 27; J. Polym. Sci., Part B: Polym. Phys., 36 (1998) 2499; J. Polym. Sci., Part B: Polym. Phys., 42 (2004) 4401.
189 483, 508, 524. M. L. Di Lorenzo, M. Pyda, A. I. Buzin, K. Matyjaszewski and B. Wunderlich, J. Polym. Sci.: Part B: Polym. Phys., 39 (2001) 1594; J. Polym. Sci.: Part B: Polym. Phys., 39 (2001) 2969; Polymer, 43 (2002) 5563.
190 367, 419, 466, 474. J. Cheng, Y. Jin, W. Chen, R. Pardey, S. Z. D. Cheng, M. Pyda, A. Habenschuss, J. D. Londono, Y. K. Kwon, B. K. Annis and B. Wunderlich, Polym. Adv. Technol., 10 (1999) 501; Polym. Adv. Technol., 8 (1997) 747; J. Polym. Sci.: Part B: Polym. Phys., 38 (2000) 319; J. Polym. Sci.: Part B: Polym. Phys., 38 (2000) 611.
191 423, 477. L. Di Lorenzo, G. Zhang, M. Pyda, B. V. Lebedev and B. Wunderlich, J. Thermal Anal., 49 (1997) 823; J. Polym. Sci., Part B: Polym. Phys., 37 (1999) 2093.
192 338. A. Xenopoulos, K. A. Roles and B. Wunderlich, Polymer, 34 (1993) 2559.
193 471. M. Pyda and B. Wunderlich, Macromolecules, 32 (1999) 2044.
194 520. M. Pyda and B. Wunderlich, J. Polym. Sci., Part B: Polym. Phys., 40 (2002) 1245.
195 W. Kauzmann, Chem. Rev., 43 (1948) 219.
196 488. G. W. H. Höhne, S. Rastogi and B. Wunderlich, Polymer, 41 (2000) 8869.
197 418, 431. A. Xenopoulos, M. Ralle, A. Habenschuss, J. C. Bryan and B. Wunderlich, Powder Diffraction, 11 (1996) 246; Acta Cryst., C53 (1997) 488.
198 405, 403. M. Pyda, M. Varma-Nair, W. Chen, H. S. Aldrich, R. H. Schlosberg, W. Chen, A. Habenschuss and B. Wunderlich, J. Thermal Anal., 46 (1996) 1093; J. Thermal Anal., 46 (1996) 1113.
199 401. M. Pyda and B. Wunderlich, J. Thermal Anal., 49 (1997) 685.
200 402, 432, 434, 446, 449, 463, 511. H. Bu, S. Shi, E. Chen, H. Hu, J. Cao, Zhensheng Zhang, Z. Zhang, S. Xu, Y. K. Kwon, R. Festag, D. C. Joy, S. D. Alexandratos, K. D. Cook, B. Annis and B. Wunderlich, J. Macromol. Sci., Phys., B35 (1996) 731; Proc. Int. Society Optical Engineering (SPIE) 2809, 155 (1996); J. Polym. Sci., Part B: Polym. Phys., 36 (1998)105; Macromolecules, 30 (1997) 6238; J. Am. Soc. Mass Spectrom., 9 (1998) 299; J. Macromol. Sci., Phys., B38 (1999) 251; Thermochim. Acta, 432 (2005) 127.
201 487, 513. I. Moon, R. Androsch, Wei Chen, A. I. Buzin, P. Kamasa, M. Pyda and B. Wunderlich, J. Therm. Anal. Cal., 59 (2000) 187; Thermochim. Acta, 381 (2002) 9.

202 530, 532, 534, 556, 570. B. Wunderlich, Thermochim. Acta, 403 (2003) 1; J. Macromol. Sci. Part B, Phys. Ed., B42 (2003) 579; J. Polym. Sci., Part B: Polym. Phys., 42 (2004) 1275; Macromol. Rapid Commun., 26 (2005) 1521; J. Appl. Polym. Sci., in print (2006).

203 535. B. Wunderlich, J. Therm. Anal. Cal., 78 (2004) 7.

204 542, 549. J. Pak, W Qiu, M. Pyda, E. Nowak-Pyda and B. Wunderlich, J. Therm. Anal. Cal., 82 (2005) 565; Thermochim. Acta, 442 (2006) 35.

205 Thermochim. Acta, 403 (2003); Thermochim. Acta, 432 (2005); Proc. 32nd NATAS Conf. in Williamsburg, VA, Oct. 4–6, M. J. Rich, Ed. CD edition, 32 (2004), Symposium on ‘Fast Scan DSC’.

206 559, 565, 572. W. Qiu, M. Pyda, E. Nowak-Pyda, A. Habenschuss and B. Wunderlich, Macromolecules, 38 (2005) 8454; J. Polym. Sci., Part B: Polym. Phys., in print (2006); Thermochim. Acta, 448 (2006) 136.

207 563. B. Wunderlich, Thermochim. Acta, 446 (2006) 128.

208 566, 571. W. Qiu, J. Sworen, M. Pyda, E. Nowak-Pyda, A. Habenschuss, K. B. Wagener and B. Wunderlich, Macromolecules, 39 (2006) 204; J. Polym. Sci., Part B: Polym. Phys., 44 (2006) 3461.

209 R. Androsch, J. Polym. Sci., Part B: Polym. Phys., 39 (2001) 750.

210 561. R. Androsch, B. Wunderlich and H.-J. Radusch, J. Therm. Anal. Cal., 79 (2005) 615.

211 568. R. Androsch and B. Wunderlich, submitted to Polymer, 46 (2005)12556.

212 558, 569. A. Habenschuss, M. Varma-Nair, Y.-K. Kwon, J. Ma and B. Wunderlich, Polymer, 47 (2006) 2369; Polymer, completed, to be submitted in 2006.

213 537, 541, 547, 557, 564. M. Pyda, R. C. Bopp, E. Nowak-Pyda, K. Van Durme, B. Van Mele and B. Wunderlich, Macromolecules, 38 (2005) 10472; J. Chem. Thermodyn., 35 (2004) 731; Proc. 32nd NATAS Conf. in Williamsburg, VA, Oct. 4–6, M. J. Rich, Ed. CD edition, 32, 10 pp., MS 165-05_401_P (2004); M. Pyda, K. Van Durme, B. Wunderlich and B. Van Mele, J. Polym. Sci., Part B: Polym. Phys., 43 (2005) 2141; Proc. 33rd NATAS Conf. in Universal City, CA, Sept. 18–21, M. J. Rich, Ed. CD edition, 33-47-550, 10 (2005). Feature Article in NATAS Notes, 37 (2005) 7.

214 562. B. Wunderlich, J. Therm. Anal. Cal., 85 (2006) 179.

215 410, 454, 567. R. Androsch and B. Wunderlich, Heat Capacity of Polymers, S. Z. D. Cheng, Ed., ‘Handbook of Thermal Analysis and Calorimetry, Vol. 3, Applications to Polymers and Plastics’; Elsevier Science, Amsterdam 2002; The Application of Modulated Temperature Differential Scanning Calorimetry to Polymer Melting, in M. Reading and D. Hourston, Eds, ‘Modulated-Temperature Differential Scanning Calorimetry’, Springer, Berlin 2006; Thermal Analysis, K. Matyjaszewski, Y. Gnanou and L. Laibler, Eds ‘Macromolecular Engineering’, Wiley-VCH, in print, 2006.

DOI: 10.1007/s10973-006-8219-5